A METHOD FOR ASTRO-GRAVIMETRIC GEOID DETERMINATION

C. L. MERRY
P. VANICEK

March 1974

PREFACE

In order to make our extensive series of technical reports more readily available, we have scanned the old master copies and produced electronic versions in Portable Document Format. The quality of the images varies depending on the quality of the originals. The images have not been converted to searchable text.

A METHOD FOR

ASTROGRAVIMETRIC GEOID DETERMINATION

by

C.L. Merry and P. Vaníček

TABLE OF CONTENTS

1) <u>Introduction</u>

The geoid is the fundamental reference surface for classical height systems, and as such, forms an essential part of any national geodetic reference system. It is also an intermediate surface for the reduction of geodetic data from the terrain to the reference ellipsoid. The geoid-ellipsoid separation (geoidal height) is not a negligible quantity in Canada and the geoid should be taken into account when reducing distances and directions to the ellipsoid [Merry and Vaníček, 1973; Merry et al., 1974]. A knowledge of the geoid is essential for the three-dimensional approach to geodetic adjustment (Krakiwsky et al., 1974) and is needed for any comparison or mutual adjustment of horizontal control networks and satellite - based networks. The geoid is also useful for the determination of the relationship between geodetic (non-geocentric) and geocentric reference systems (Merry and Vaníček, 1974).

The geoid, as related to a geodetic reference ellipsoid, is computed from the astro-geodetic deflections of the vertical (fig. 1.1) Such a geoid is called an astrogeodetic geoid. The conventional integration technique is by line integrals along geodetic triangulation chains. A surface-fitting technique has been developed and tested at the University of New Brunswick (Vaníček and Merry, 1973)
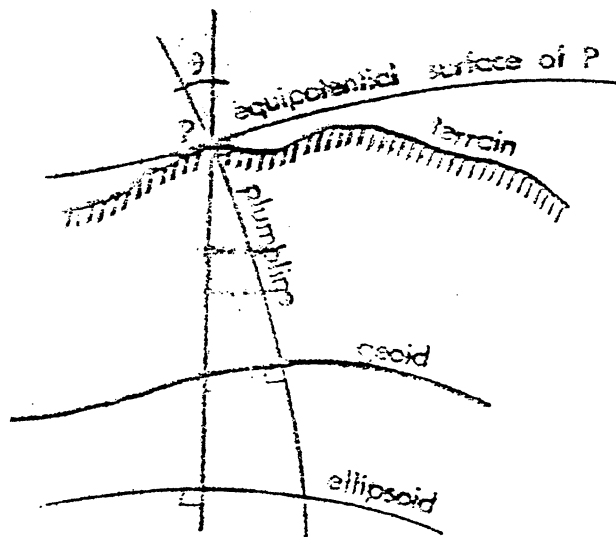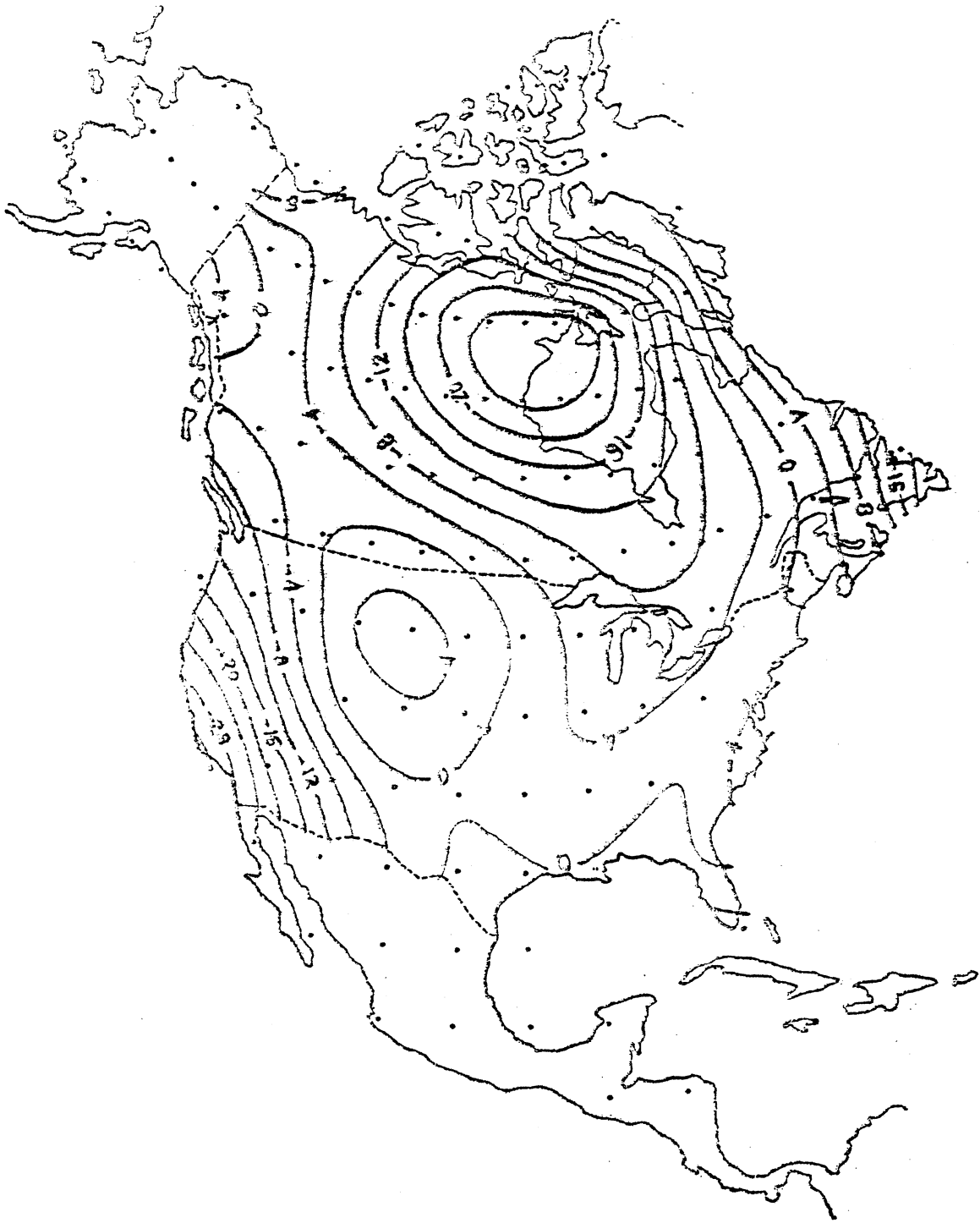
Fig. 1.1 Deflection of the vertical and the geoid

Fig. 1.2 Astrogeodetic Geoid
in North America

and a preliminary astrogeodetic geoid for North America computed
(fig 1-2). This technique forms the basis for the method described
in this report.

The astro-geodetic deflection coverage in Canada is
rather sparse (fig. 1.3), and thus the geoid based on these deflections
is unreliable in many regions. Attempts are being made to improve
this coverage (Dept. of Energy, Mines and Resources, 1972) but the
improvement will be a long, slow and costly process. An alternative
approach, advocated by Molodenskii (Molodenskii et al, 1962) is to
use observed gravity in combination with astrogeodetic deflections,
to produce a so-called astrogravimetric geoid. This geoid is also
referred to the geodetic reference ellipsoid, but is more reliable
and more detailed than the astrogeodetic geoid. The usual approach
is to use the gravity data to compute modified gravimetric deflections
via the Vening-Meinez integration formulae (Vening-Meinez, 1928). The
available astrogeodetic deflection data is then used to transform these
modified gravimetric deflections to the geodetic datum, producing inter-
polated astrogeodetic deflections. These interpolated deflections
can be used on their own for azimuth control or angle reductions, or
they can be used, together with the original astrogeodetic deflections
as the basic data for the computation of the astro-gravimetric geoid.
The technique outlined above has been tested for a region in New
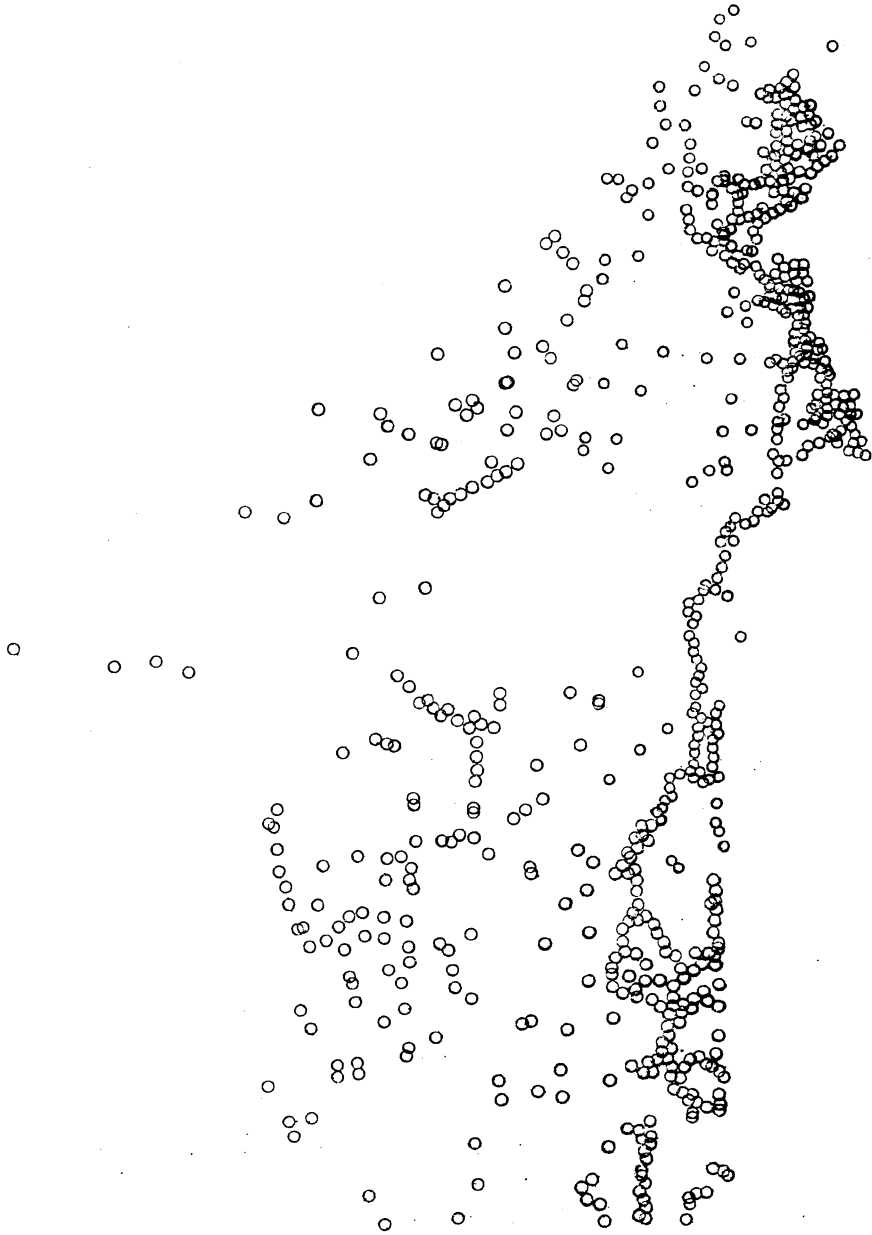Brunswick and the results of this test are discussed in the last
chapter.

Fig. 1.3 Astrogeodetic Deflections in Canada

2) <u>Gravimetric Data</u>

Well over 150,000 gravity observations have been made in Canada, and a very large proportion of these have been connected to the Canadian Gravity Net and are available in the files of the Earth Physics Branch (EPB). Gravity anomalies, both free-air and Bonguer, have been computed based upon the 1930 International Gravity formula from these observations (Buck and Tanner, 1972). The present status of the free-air gravity anomaly coverage is shown in (Nagy, 1973) where 104,311 free-air anomalies were used to compute a free-air anomaly map of Canada. Significant gaps still exist in British Columbia, the Yukon Territory and Northern Labrador.

No estimates are readily available for the accuracy of the point gravity anomalies. The errors in the gravity anomalies are primarily a function of the measurement errors and the height error. The measurement error is estimated to be 0.05 mgal. (Vaniček et al., 1972), and is the smaller of the two. The remainder is due to the error in height (the gravity anomalies are only weakly dependent upon horizontal position) and the procedure given in (Vaniček et al., 1972) has been used to estimate the accuracy of the gravity anomalies from the height errors of the observations. The resultant values are shown in table 2-1 where $\sigma_{\Delta g}$, the standard error of an anomaly Δg is given as a function of ΔH, the estimated height error.

$\sigma_{\Delta g}$ (mgals.)	ΔH (feet)
0.05	0.1
0.1	1.0
0.3	3.0
0.9	10.0
2.4	25.0
9.4	100.0
12.0	unknown

Table 2.1: $\sigma_{\Delta g}$ (standard error of a gravity anomaly) as a function of ΔH (estimated height error).

As described in the next chapter, besides point gravity
anomalies, mean values for surface elements (blocks) with sides of
1° and 1/3° respectively, are also needed. The 1° x 1° data is readily
available. Means have been computed by the E.P.B. for 2,131 one degree
blocks (really, spherical trapezoids) in Canada (J. G. Tanner, pers.
comm, 1973). An additional 20,113 one degree square values for the
whole earth have been obtained from the Defense Mapping Agency (DMA)
in St. Louis, Missouri (W. Durbin, pers. Comm., 1972)

For the purpose of carrying out the Vening-Meinesz inte-
gration, the knowledge of mean gravity anomalies is required outside
Canadian territory. Consequently, the two data sets mentioned above
were combined into one, for the region bounded by latitudes 40° and
85° N, and longitudes 50° W and 150° W. There are some overlaps of
data in the original files, notably along the common border of Canada
and the U.S.A., and for these instances, the weighted mean of the
two values for each overlapping degree square was adopted. The original
error estimates for the EPB data are somewhat optimistic being based
on the deviation of point values from the mean. In order to make the
set of error estimates as homogeneous as possible, standard errors
have been assigned to the EPB data in accordance with the procedure
described in (Rapp, 1972). Rapp obtained an empirical correlation
between the DMA error estimates and the number of data points per
1° x 1° block, which is shown diagrammatically in Fig. 2.1. The
weights used in the combination of common blocks were inversely
proportional to the squares of the assigned standard errors.

Fig. 2.1 Error function - 1° x 1° blocks
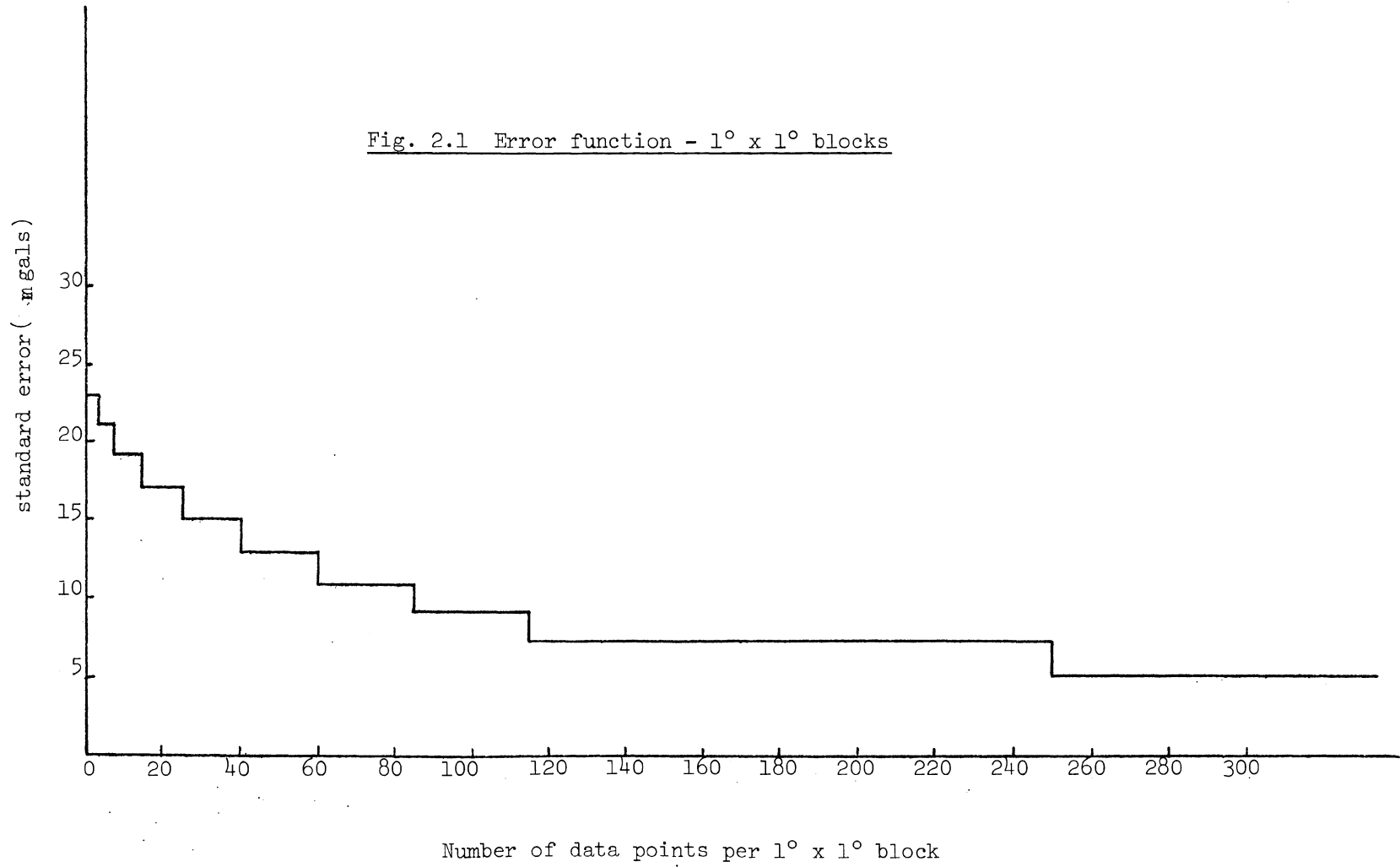
The combination of the two data sets in one set of 3311 (1° x 1°) blocks still left some empty areas in Canada, notably in Northern British Columbia, the Yukon and portions of the Northwest Territories. An additional 1322 mean anomalies were predicted for these areas, using a simple geometric interpolation procedure. For a block with centre co-ordinates (latitude and longitude) of ϕ_p, λ_p, the mean anomaly $\hat{\Delta g}_p$ is predicted from the values Δg_i in the neighbouring blocks, using the following formula:

$$\hat{\Delta g} = \frac{\sum\limits_i \Delta g_i w(\psi_i)}{\sum\limits_i w(\psi_i)} \qquad i = 1, \ldots n \qquad 2.1$$

where the weight function is specified as

$$w(\psi_i) = \sigma_{\Delta g_i}^{-2} \; e^{-\psi_i/1.5°} \qquad i = 1, \ldots n \qquad 2.2$$

Here, $\sigma_{\Delta g_i}$ is the standard error of Δg_i, and ψ_i is the angular distance (in degrees) between the points (ϕ_p, λ_p) and (ϕ_i, λ_i). Without the exponential term the above expressions would represent a simple weighted arithmetic mean. However, the correlation of gravity anomalies decreases with distance, and this should be taken into account when predicting mean anomalies. The correlation is non-linear and is best represented by an exponential function (Kaula, 1957), of the form used above. The value 1.5° has been taken from the same publication, in which Kaula uses several gravity profiles in the U.S.A. to determine correlation coefficients for mean free-air gravity anomalies. Estimates of the accuracy of the predicted gravity anomalies are found from:

$$\sigma_{\hat{\Delta g}_p}^2 = (\sigma_o^2 + \frac{\sum\limits_i \sigma_{\Delta g_i}^2}{n}) \qquad 2.3$$

where;

$$\sigma_o^2 = \frac{\sum\limits_i (\tilde{\Delta g}_p - \Delta g_i)^2 \cdot w(\psi_i)}{(n-1) \ \Sigma w(\psi_i)}$$ 2.4

Equation 2.4 represents the least squares estimate of the standard error of the mean [Krakiwsky and Wells, 1971] and is based upon the premise that:

$$\tilde{\Delta g} = E \ (\Delta g_i)$$ 2.5

where E represents the expectation operator.

This premise is no longer valid in the case of gravity prediction, where, the mean, $\tilde{\Delta g}$ does not represent the expected value of individual anomalies. In order to take into account the standard errors of the surrounding gravity blocks, a mean value for these quantities is used in equation 2.3. Although, from a rigorous statistical point of view, this technique is questionable, it does avoid the practical difficulty of computing large error covariance matrices required for the more rigorous approach advocated in, for example, (Moritz, 1972).

The blocks used for the prediction are those immediately adjacent to the empty block ($\psi_{max} = 1°.5$). If there are less than two blocks with known anomalies available in the adjacent area, ψ_{max} is increased to $3°.0$, and then to $4°.5$. If there are less than two blocks within $4°.5$ of (ϕ_p, λ_p), no attempt is made to search any further, and no value is calculated for that particular empty block. However, we were able to predict anomalies so that observed and predicted ($1° \times 1°$) values are now available for the entire land mass of Canada and the immediately adjacent areas, both on land and sea (fig. 2.2).
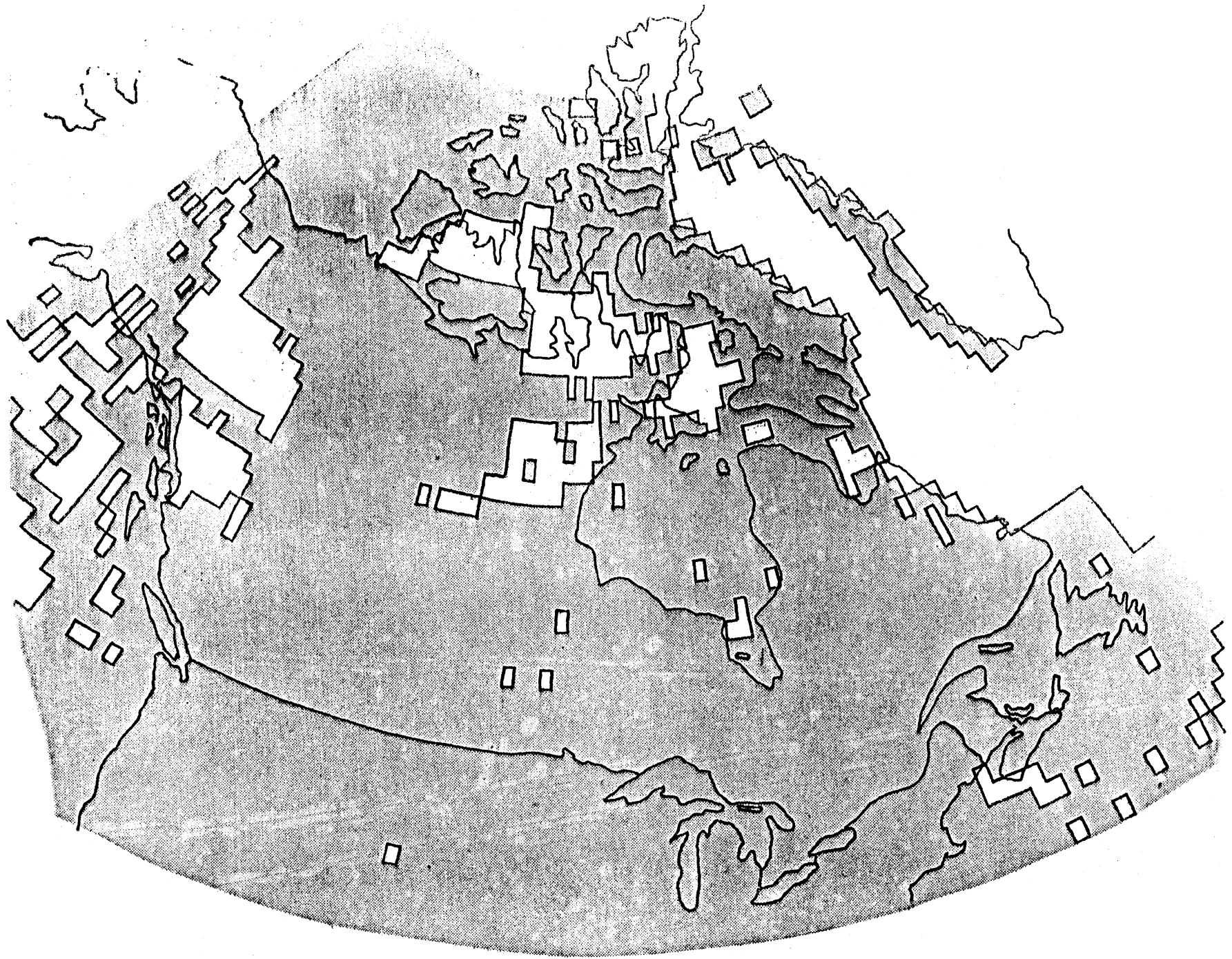
Fig. 2.2 1°x 1° mean free air gravity anomalies

- observed

The determination of ($1/3°$ x $1/3°$) mean anomalies is a more complex one, as they have to be found from the point gravity data. The selection of ($1/3°$ x $1/3°$) as the optimum size is based on the requirement for smaller blocks in the vicinity of the computation point when the Vening-Meinesz equations are used (chapter three). An even smaller block size would have been desirable, but the selection is limited by the density of the point data available for the computations. The EPB plans are for an eventual optimum density of one gravity station per 10 km to 15 km. (Nagy, 1974), which would result in 9 to 16 point values within each ($1/3°$ x $1/3°$) block - just sufficient for a reliable estimate of the mean value to be made. Any smaller block size would result in too few point values per block.

The mean gravity anomaly Δg for a region is given by:

$$\overline{\Delta g} = \frac{1}{A} \iint \Delta g \quad dA \qquad\qquad 2.6$$

(Heiskanen and Moritz, 1967)

where A is the area of the region and Δg is the gravity anomaly known at every point in the region. In practice, the anomalies are only measured at a few points in the region and the complete evaluation of the surface integral is not possible. However, if there is sufficient data, the gravity anomalies in the region can be approximated by fitting a polynomial to the observed data (Nagy, 1963). Then for any point i:

$$\widetilde{\Delta g}_i = c_{00} + c_{01}y_i + c_{02}y_i^2 + c_{10}x_i + c_{11}x_i y_i + c_{12}x_i y_i^2 + c_{20}x_i^2 + c_{21}x_i^2 y_i + c_{22}x_i^2 y_i^2$$

where (x,y) is a local orthogonal coordinate system.

This polynomial can then be numerically integrated using 100 symmetrically distributed elements and divided by the area, to determine the mean, $\overline{\Delta g}$. The coefficients of this polynomial are found from a least-squares approximation procedure: (Vaníček and Wells, 1972)

$$\sum_{j=1}^{9} < \phi_k, \phi_j > c_j = < \Delta g, \phi_k > \qquad k=1,\ldots 9 \qquad 2.8$$

where: $\phi_1(x_i, y_i) = 1$, $\phi_2(x_i, y_i) = y_i$, $\phi_3(x_i, y_i) = y_i^2, \ldots \phi_9(x_i^2, y_i^2) = x_i^2, y_i^2$

and the scalar product $< \phi_k, \phi_j >$ is defined by:

$$< \phi_k, \phi_j > = \sum_{i=1}^{n} W(x_i, y_i) \cdot \phi_k(x_i, y_i) \cdot \phi_j(x_i, y_i) \quad 2.9$$

where n = number of data points used.

The weight function $W(x_i, y_i)$ is given as:

$$W(x_i, y_i) = \sigma_{\Delta g_i}^{-2} \qquad 2.10$$

where $\sigma_{\Delta g_i}$ is the standard error of the point gravity anomaly, Δg_i.

Equations 2.8 can be written in the matrix form:

$$G \underset{\sim}{c} = \underset{\sim}{\ell} \qquad 2.11$$

from which:

$$\underset{\sim}{c} = G^{-1} \underset{\sim}{\ell} \qquad 2.12$$

Residuals can be computed for the observed data points:

$$v_i = \Delta g_i - \tilde{\Delta g}_i \qquad 2.13$$

where $\tilde{\Delta g}_i$ is given by equation 2.7.

Then the variance factor σ_o^2 is determined from:

$$\sigma_o^2 = \frac{\sum\limits_{i=1}^{n} v_i^2 \ W \ (x_i y_i)}{n-9} \qquad 2.14$$

The error covariance matrix of the coefficients is then:

$$\Sigma_c = \sigma_o^2 \ G^{-1} \qquad 2.15$$

Applying the theory of propagation of covariance (Vanicek, 1973) the error covariance matrix for the 100 integration elements, $\overset{\sim}{\Delta g}_k$ is:

$$\Sigma_{\Delta g_k} = B_1 \ \Sigma_c \ B_1^T \qquad 2.16$$

where B_1 is a linear operator on the coefficients to get Δg_k (defined by equation 2.7). The propagation can be carried one step further, to determine the standard error, $\sigma_{\overline{\Delta g}}$, of the mean gravity anomaly:

$$\sigma_{\overline{\Delta g}} = B_2 \ \Sigma_{\overset{\sim}{\Delta g}_k} \ B_2^T \qquad 2.17$$

where B_2 is a linear operator on the $\overset{\sim}{\Delta g}_k$, to get the mean anomaly, $\overline{\Delta g}$ given by equation 2.6.

The procedure described above has been used for computing some ($1/3^\circ$ x $1/3^\circ$) mean gravity anomalies. It is not possible to use this procedure for all cases, as there is not always sufficient well-distributed point gravity data within individual ($1/3^\circ$ x $1/3^\circ$) blocks. Practical experience has indicated that there should be at least 50% more data points than unknowns for a stable solution for the polynomial coefficients. As well, there should be at least one data point per quadrant.

If this condition is not fulfilled and there are less than 15 data points in the block, the weighted arithmetic mean of the point gravity anomalies is used to represent the mean anomaly of the block. The weights used are inversely proportional to the variances of the available anomalies. As mentioned earlier, the mean value of a block is not the expected value of the individual point anomalies, and the standard deviation of the mean of the sample should not be used as a measure of the accuracy of the mean. Thus, we had to devise another technique to get a less biased estimate for the accuracy. The rigorous integral approach can be used to solve this problem. Where the standard deviation of the integral solution is plotted against the number of points one discovers that there is a strong quadratic correlation apparent. Hence one can use this second order curve (see fig. 2.3) to predict the standard deviation for the blocks that have less than 15 points, i.e. those blocks for which the straight mean is employed. These predicted standard deviations are then used instead of the biased ones.

By the methods outlined above, 2432 ($1/3°$ x $1/3°$) mean gravity anomalies for Eastern Canada have been calculated. However, many blocks still exist in which no data has been observed at all. For these regions, predicted values have been calculated using the same techniques as described earlier for the ($1°$ x $1°$) blocks. Again, the blocks used for the prediction are the immediately adjacent ones (ψ_{max}= $0°.5$). If there are less than two "observed" adjacent blocks, then ψ_{max} is increased to $1°.0$ and $1°.5$. If there are still less than two blocks in the region,

Fig. 2.3 Error function - 1/3° x 1/3° blocks

Standard error (m gals)
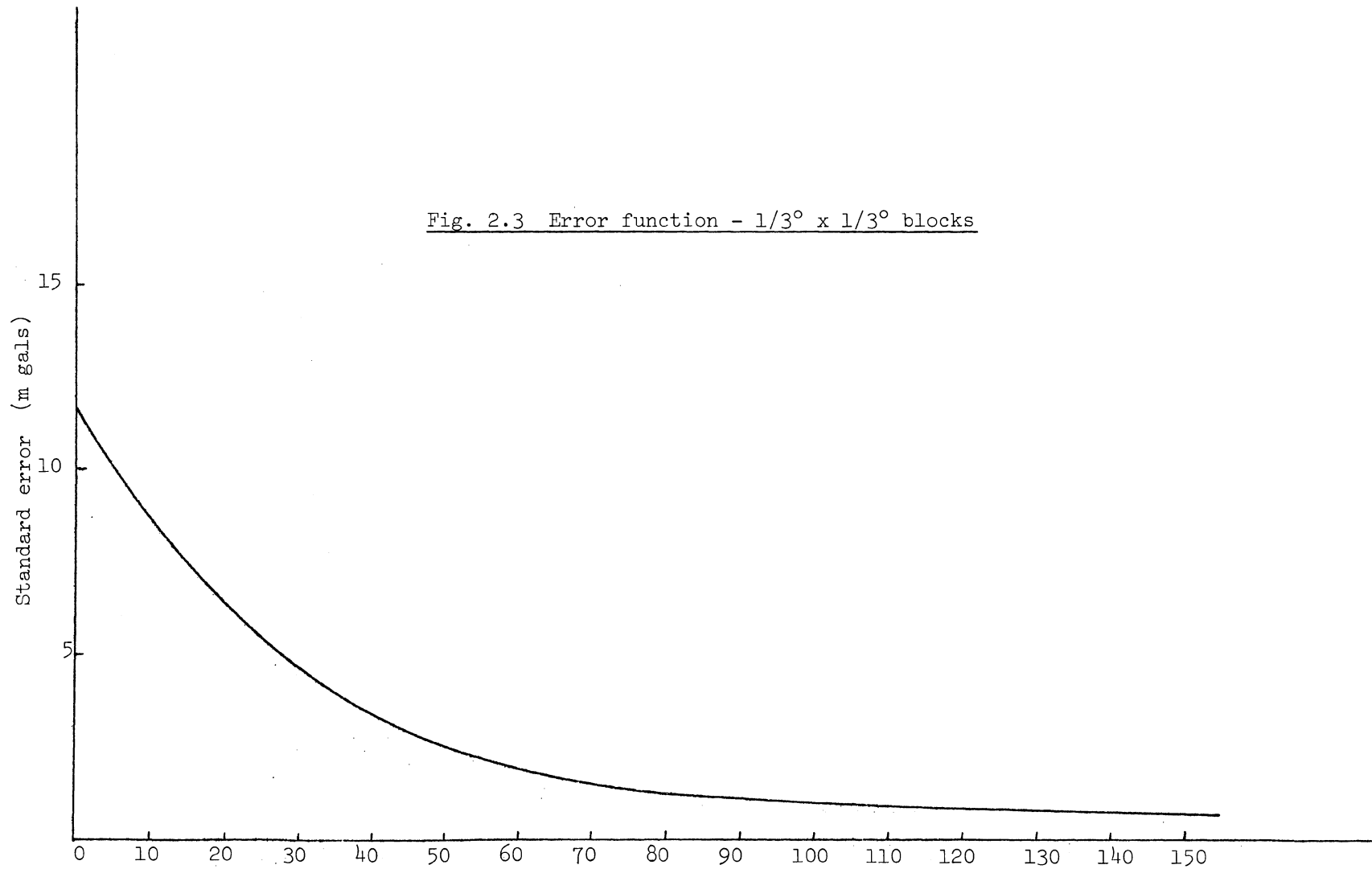
Number of data points per 1/3° x 1/3 block

then no predicted value is determined. For Eastern Canada and the
North-east United States there were 1051 empty blocks for which values
have been predicted. Thus the total coverage in this region is 3483
blocks of "observed" and predicted mean anomalies. The ($1/3°$ x $1/3°$)
observed and predicted coverage in New Brunswick and adjacent areas is
shown in figure 2.4.

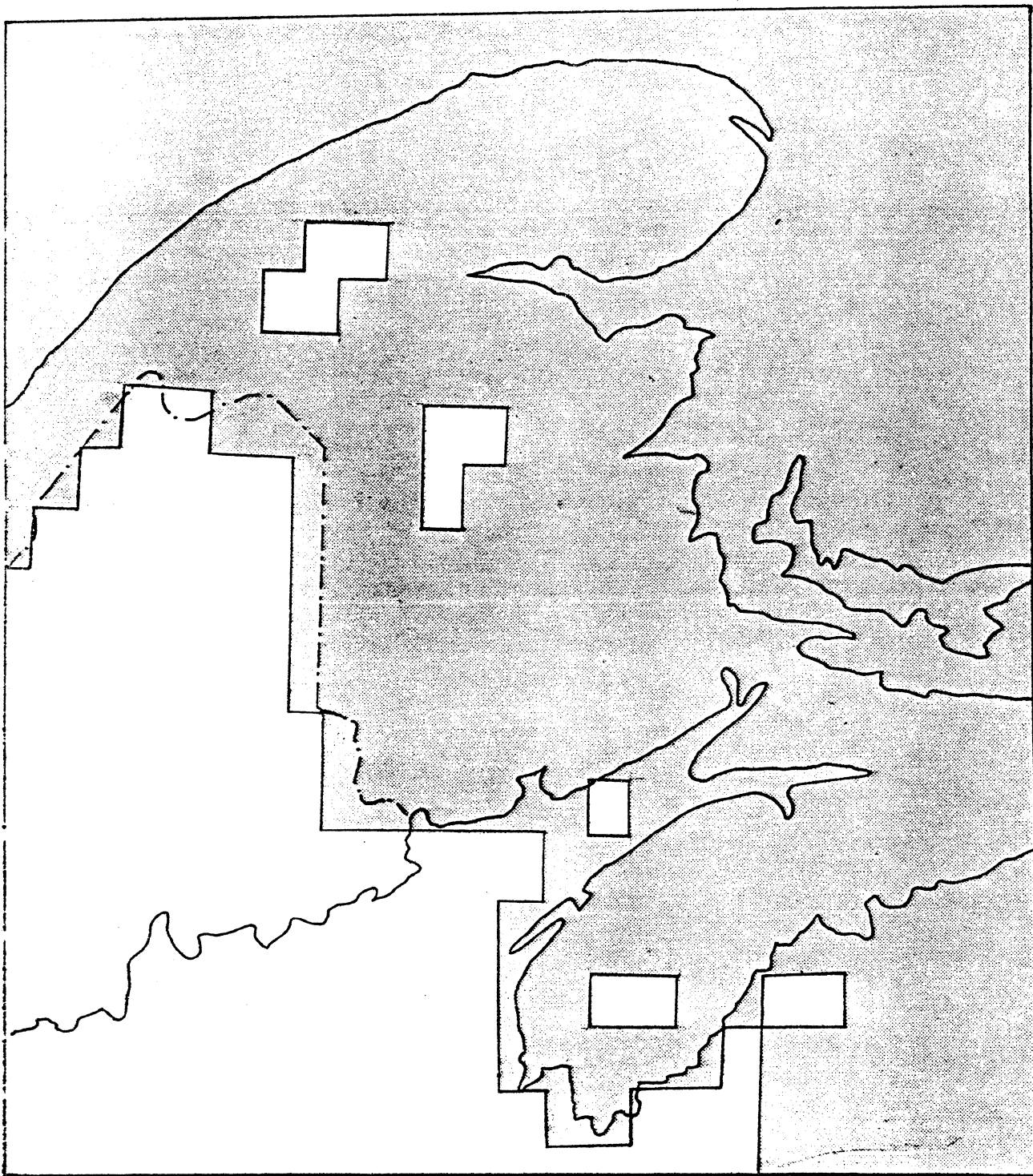Fig. 2.4   Gravity Anomaly Coverage in New Brunswick and Vicinity

- area in which there is at least one anomaly

per 1/3° x 1/3° block

3) <u>Gravimetric Deflections</u>

A Gravimetric deflection of the vertical is the angle

between the actual plumbline and the normal to a geocentric reference

ellipsoid, measured at the geoid. The value of the deflection will

depend upon the particular size and shape parameters of the geocentric

ellipsoid used for generating normal gravity. In this report, all data

used is referenced to the International Gravity formula (1930), based

upon the International Ellipsoid of Hayford (Heiskanen and Moritz, 1967).

The two components of the deflection in meridian and the prime vertical

are denoted by ξ^G, η^G. The superscript, G, is used to distinguish them

from the corresponding astrogeodetic deflections ξ^A, η^A. As mentioned

earlier gravimetric deflections are computed by means of the integration

formulae developed by the Dutch geodesist, F. A. Vening-Meinesz

(Vening-Meinesz, 1928). Essentially, the components are the spatial

derivatives of Stoke's formula for geoidal heights (G. G. Stokes, 1849).

The classical theory of the gravity potential of the earth, leading to

these equations is described in several texts (see, for instance,

Heiskanen and Moritz, 1967) and will not be discussed here. The formulae

of Vening-Meinesz are:

$$\xi^G = \frac{1}{4\pi G} \iint_{\sigma} \Delta g \, \frac{dS(\psi)}{d\psi} \cos \alpha \, d\sigma$$

$$\eta^G = \frac{1}{4\pi G} \iint_{\sigma} \Delta g \, \frac{dS(\psi)}{d\psi} \sin \alpha \, d\sigma \qquad\qquad 3.1$$

where the symbols have the following meanings:

ξ^G, η^G are the gravimetric deflections of the vertical

$\pi = 3.141592653\ldots$

G is an average value of gravity on the surface of the earth

Δg is a gravity anomaly

$$\frac{dS(\psi)}{d\psi} = \frac{-\cos(\psi/2)}{2 \sin^2(\psi/2)} + 8 \sin \psi - 6 \cos (\psi/2) - 3 \frac{1-\sin(\psi/2)}{\sin \psi}$$

3.2

$$+ 3 \sin \psi \ln [\sin (\psi/2) + \sin (\psi/2)]$$
(Vening-Meinesz function)

ψ is the spherical distance from the computation point to the particular gravity anomaly, and α is the azimuth of the line connecting the computation point with the point at which Δg is taken.

The integration is a closed integration and has to be carried out over the surface of the whole earth. In practice, it is sufficient to integrate over the surface of a sphere which has the same volume as the earth. The practical application of these formulae require the replacement of the integration by a summation over finite elements:

$$\xi^G = \frac{1}{4\pi G} \Sigma \Sigma \Delta g \frac{dS(\psi)}{d\psi} \cos \alpha \, d\sigma$$

$$\eta^G = \frac{1}{4\pi G} \Sigma \Sigma \Delta g \frac{dS(\psi)}{d\psi} \sin \alpha \, d\sigma$$

3.3

Molodensky's idea (Molodensky et al, 1962), of using the Vening-Meinesz formulae is based on the following observation. When

we compute the gravimetric deflections ξ^G, η^G in a confined region

the influence of the distant elements (distant gravity anomalies) varies

only very slowly from point to point. Hence, if one carries out the

Vening-Meinesz integration or the corresponding double summation over

just a sufficiently large vicinity of the region of interest, one

obtains some modified gravimetric deflections that differ from the

correct gravimetric deflections by an almost constant value. Then this

difference can be treated as part of the correction that has to be

applied to convert the gravimetric deflections (related to a geocentric

ellipsoid) to astro-geodetic deflections (related to the geodetic

ellipsoid). Thus, for our purpose, the equation 3.3. will be always

evaluated just over the vicinity of the region of interest.

There are two techniques of computing the deflections from

equation 3.3. commonly used. One uses elements that are portions of

discs, centered at the computation point P, i.e. "circular" coordinates

on the suface of the earth (fig. 3.1a). The other uses quasi-rectangular

blocks formed by the intersections of meridians and parallels, i.e.

"rectangular" coordinates on the surface of the earth (fig. 3.1b).
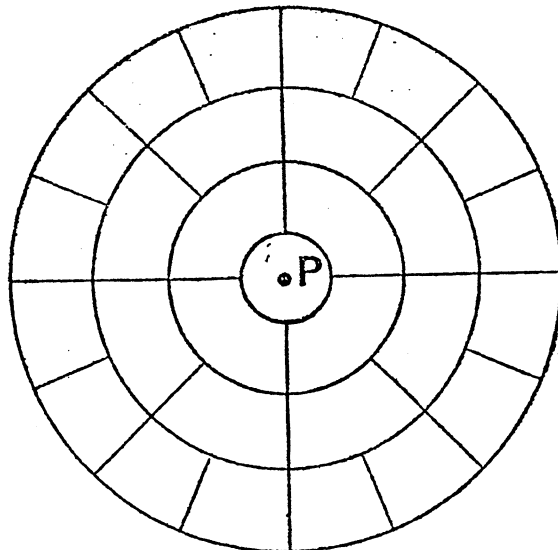
Fig. 3.1a Circular Templates
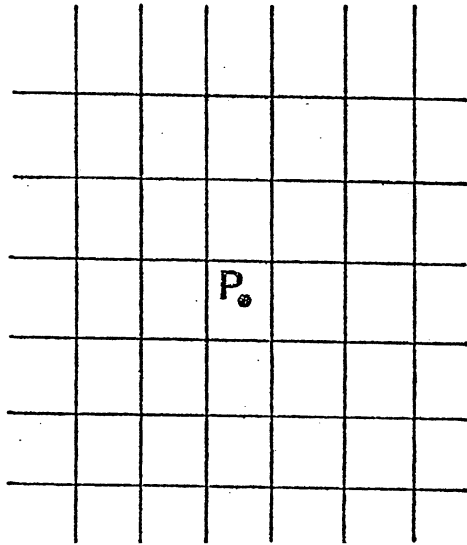
Fig. 3.1b Rectangular Blocks

Both methods require the calculation of mean values of Δg for each element. However, when the circular elements are used, the values of Δg must be recomputed every time the computation point, i.e. the centre of the coordinates, is moved. The rectangular block mean values do not change with the computation point, and can be precomputed, stored and used repeatedly. The first method was originally useful when access to high-speed computers was difficult or impossible, and circular transparent templates were used in conjunction with contour maps of gravity anomalies (e.g. Rice 1952, Derenyi, 1965). This work required a great deal of

time, and very few deflections were calculated.

The use of rectangular blocks for computation of deflections of the vertical is described in Uotila (1960) where the author recommends a combination of blocks and circular templates, the templates to be used for the inner area, and blocks of (1° x 1°) and (5° x 5°) size to be used for the outer areas.

This technique has been used for computing gravimetric deflections of the vertical in North America by Nagy (1963) and Fischer (1965). However their methods allow gravimetric deflections to be computed only at block corners, or at the geometric centres of blocks. Fischer overcomes this problem by computing "curvature" components (spatial derivatives of the deflections) and using these to interpolate deflections at any point. This technique requires a uniform, dense, gravity coverage in the vicinity of the computation point, and would therefore not be feasible for Canadian conditions.

A more general approach, involving an analytical solution for the deflections in the immediate vicinity of the computation point, and a series approximation for the gravity field in this vicinity, has been developed here. The summation in equation 3.3 is broken into three parts:

$$\xi^G = \xi_1 + \xi_2 + \xi_3$$
$$\eta^G = \eta_1 + \eta_2 + \eta_3$$

3.4

where each of the subscripted values is determined from a different region and incorporates different block sizes (fig. 3.2). The block sizes used are (1° x 1°) blocks, for the outer zone, and (1/3° x 1/3°)

blocks for the middle zone.
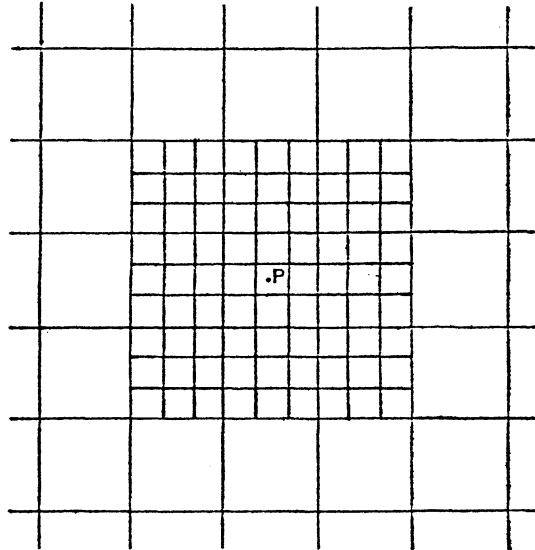
Fig. 3.2 Different-sized Rectangular Blocks

The choice of ($1°$ x $1°$) blocks was predetermined by the fact that these were the smallest blocks for which mean values were readily available (see the report by Decker (1972) for a description of data available). The Vening-Meinesz function $\frac{dS(\psi)}{\psi}$ goes to infinity at the computation point (fig. 3.3) and it is evident that even smaller elements should be used for the immediate vicinity of the computation point. A ($1/3°$ x $1/3°$) size has been chosen as a compromise between a theoretically preferable smaller block size and the practical fact that the available gravity data in Canada has a density of one point per 10 km or less. The innermost ($1/3°$ x $1/3°$) in which the computation point is contained is treated in a different way, using point data to determine the coefficients of a truncated Taylor series for the gravity anomalies. The analytical expression for the integration of this series has been derived, using approximations for

the Vening-Meinesz function, as we shall show later.

The determination of each of the components is outlined below:

(i) Evaluation of ξ_1, η_1

First we rewrite the part of eqn. 3.3 pertinent to the outer zone as follows:

$$\xi_1 = \frac{1}{4\pi G} \sum_{i=1}^{n} \overline{\Delta g}_i \left(\frac{dS(\psi)}{d\psi}\right)_i \cos \phi_i \cos \alpha_i d\phi_1 d\lambda_1$$

$$\eta_1 = \frac{1}{4\pi G} \sum_{i=1}^{n} \overline{\Delta g}_i \left(\frac{dS(\psi)}{d\psi}\right)_i \cos \phi_i \sin \alpha_i d\phi_1 d\lambda_1$$

3.5

where: $\overline{\Delta g}$ is the mean value of the gravity anomaly in the ith block, $\left(\frac{dS(\psi)}{d\psi}\right)$ is evaluated at the mid-point of the ith block, ϕ_i is the latitude of the mid-point, $d\phi_1 = d\lambda_1 = 1°$ and ψ_i, α_i are given by:

$$\psi_i = \text{arc cos } (\sin\phi_p \sin \phi_i + \cos \phi_p \cos \phi_i \cos (\lambda_i - \lambda_p))$$

$$\alpha_i = \text{arc tan } \left(\frac{\cos \phi_i \sin (\lambda_i - \lambda_p)}{\cos \phi_p \sin \phi_i - \sin \phi_p \cos \phi_i \cos(\lambda_i - \lambda_p)}\right)$$

This summation is only carried out over the outer region, not covered by the $1/3° \times 1/3°$ and point gravity data.

(ii) Evaluation of ξ_2, η_2

The part of eqn. 3.3 pertinent to the middle zone is similarly given by:

$$\xi_2 = \frac{1}{4\pi G} \sum_{j=1}^{m} \Delta g_j \left(\frac{dS(\psi)}{d\psi}\right)_j \cos \phi_j \cos \alpha_j d\phi_2 d\lambda_2$$

$$\eta_2 = \frac{1}{4\pi G} \sum_{j=1}^{m} \Delta g_j \left(\frac{dS(\psi)}{d\psi}\right)_j \cos \phi_j \sin \alpha_j d\phi_2 d\lambda_2$$

3.6

where: $d\phi_2 = d\lambda_2 = 1/3°$, and the other symbols have the same

meanings as before. The summation is carried out over the

(1/3° x 1/3°) blocks in the middle zone, excluding the innermost

(1/3° x 1/3°) block.

For the (1/3° x 1/3°) blocks near the computation point,

it is no longer valid to use a value of $\frac{dS(\psi)}{d\psi}$, evaluated at the

centre of each block, due to the rapid change in this function

near the computation point (fig. 3.3). A more rigorous approach

is to integrate $\frac{dS(\psi)}{d\psi}$ over the block:

$$\overline{\frac{dS(\psi)}{d\psi}} = \frac{1}{A} \iint\limits_A \frac{dS(\psi)}{d\psi} \, da \qquad\qquad 3.7$$

where $\overline{\frac{dS(\psi)}{d\psi}}$ denotes the mean value of $\frac{dS(\psi)}{d\psi}$ for the block, and

A is the block area. For those blocks within 0°.5 of the computation

point, equation 3.7 (with a numerical integration) is used instead

of the value for $\frac{dS(\psi)}{d\psi}$ at the centre of the block. When the

computation point is at, or very close to the edge of its own

(1/3° x 1/3°) block, the numerical integration breaks down, as

$\frac{dS(\psi)}{d\psi}$ tends to infinity. The practical solution to this has been

to change the co-ordinates of the computation point slightly so

that it is at least 0°.01 away from the edge. The remaining error

due to the numerical integration is then estimated to be less than

10% of the deflection value (Table 3.1).
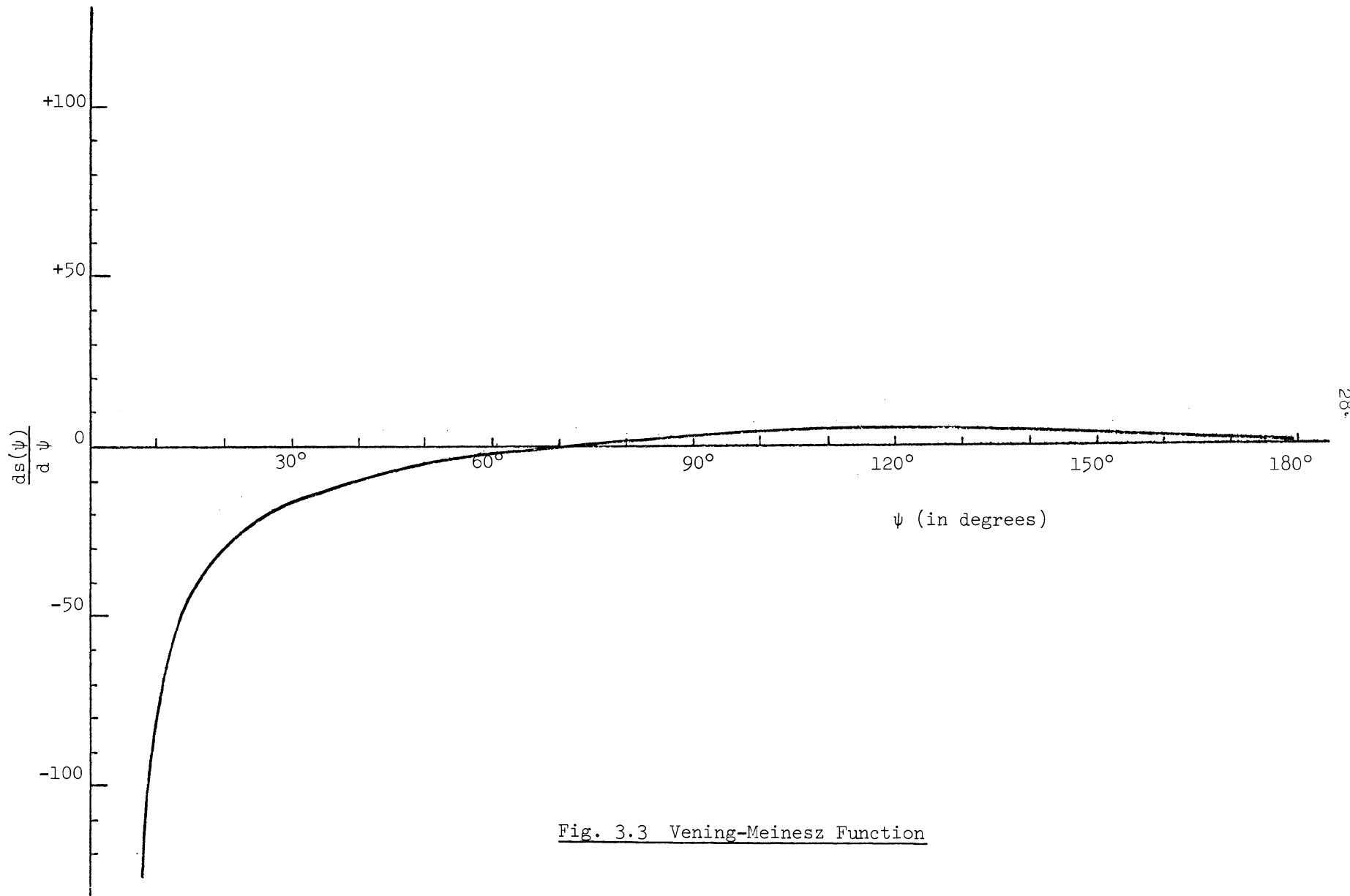
Fig. 3.3 Vening-Meinesz Function

For $\bar{\Delta}g$ = 50 mgal in adjacent block.

Angular distance from computation point to edge of block.	Contribution to deflection.	Error (seconds of arc)	Error (percentage)
0°17	1".32	0".01	1
0°10	2".38	0".03	1
0°07	3".30	0".05	2
0°04	5".03	0".18	4
0°02	7".44	0".51	7
0°01	8".95	0".90	10
0°001	13".80	3".20	23

Table 3.1. Error in numerical integration of $\dfrac{dS(\psi)}{d\psi}$ for $(1/3° \times 1/3°)$ blocks adjacent to block containing computation point.

(iii) Evaluation of ξ_2, n_3

The contribution of the inner ($1/3° \times 1/3°$) block is given by:

$$\xi_3 = -\frac{1}{2\pi G}(\Delta g_p \cdot f_1 + g_x f_2 + g_y f_3) - \frac{3}{4\pi GR}(\Delta g_p g_1 + \frac{1}{2}g_x g_2 + \frac{1}{4}g_y g_3)$$

$$n_3 = \frac{1}{2\pi G}(\Delta g_p \cdot f_1' + g_y f_2' + g_x f_3') - \frac{3}{4\pi GR}(\Delta g_p g_1' + \frac{1}{2}g_y g_2' + \frac{1}{4}g_x g_3') \qquad 3.9$$

where: Δg_p is the gravity anomaly at the computation point p, and

g_x, g_y are the horizontal gradients of gravity at p, evaluated

in an (x, y) local plane co-ordinate system in which the x-axis

is directed North, the y-axis East, and the origin is at p.

R is a mean radius of curvature for the earth and:

$$f_1 = \ln(y_2 + \sqrt{(x_1^2 + y_2^2)}) - \ln(y_2 + \sqrt{(x_2^2 + y_2^2)}) - \ln(y_1 + \sqrt{(x_1^2 + y_1^2)}) + \ln(y_1 + \sqrt{(x_2^2 + y_1^2)})$$

$$f_2 = y_2\ln(x_2 + \sqrt{(x_2^2 + y_2^2)}) - y_2\ln(x_1 + \sqrt{(x_1^2 + y_2^2)}) - y_1\ln(x_2 + \sqrt{(x_2^2 + y_1^2)}) + y_1\ln(x_1 +$$
$$+ \sqrt{(x_1^2 + y_1^2)})$$

$$f_3 = \sqrt{(x_1^2 + y_2^2)} - \sqrt{(x_2^2 + y_2^2)} - \sqrt{(x_1^2 + y_1^2)} + \sqrt{(x_2^2 + y_1^2)}$$

$$g_1 = \frac{1}{2}(y_2\ln(x_2^2 + y_2^2) + y_1\ln(x_1^2 + y_1^2) - y_2\ln(x_1^2 + y_2^2) - y_1\ln(x_2^2 + y_1^2)) + x_2\tan^{-1}\frac{y_2}{x_2}$$

$$+ x_1\tan^{-1}\frac{y_1}{x_1} - x_2\tan^{-1}\frac{y_1}{x_2} - x_1\tan^{-1}\frac{y_2}{x_1} \qquad 3.10$$

Fig. 3.4 Inner zone - **x,** y co-ordinates

$$g_2 = x_2y_2 - y_2^2\tan^{-1}\frac{x_2}{y_2} + x_2^2\tan^{-1}\frac{y_2}{x_2} - x_1y_2 + y_2^2\tan^{-1}\frac{x_1}{y_2} - x_1^2\tan^{-1}\frac{y_2}{x_1} - x_2y_1$$

$$+ y_1^2\tan^{-1}\frac{x_2}{y_1} - x_2^2\tan^{-1}\frac{y_1}{x_2} + x_1y_1 - y_1^2\tan^{-1}\frac{x_1}{y_1} + x_1^2\tan^{-1}\frac{y_1}{x_1}$$

$$g_3 = (x_2^2+y_2^2)\ln(x_2^2+y_2^2) - (x_1^2+y_2^2)\ln(x_1^2+y_2^2) - (x_2^2+y_1^2)\ln(x_2^2+y_1^2) + (x_1^2+y_1^2)\ln(x_1^2+y_1^2)$$

The equations for the primed quantities are identical to those above, except that the x and y co-ordinates are interchanged. x_1, y_1, x_2, y_2 are the co-ordinates of the four corners of the innermost (1/3° x 1/3°) block, relative to the point p (fig. 3.4). Equations 3.9 and 3.10 are derived in appendix A. Values for Δg_p, g_x, g_y are found by fitting a plane to the point gravity data in the innermost block. The plane is defined by the following expression:

$$\Delta g_i = \Delta g_p + g_x \bigg|_p x_i + g_y \bigg|_p y_i \qquad\qquad 3.11$$

a truncated series expansion at p. Putting:

$$c_1 = \Delta g_p; \quad c_2 = g_x; \quad c_3 = g_y; \quad \phi_1 = 1; \quad \phi_2 = x; \quad \phi_3 = y$$

$$\Delta g_i = c_1\phi_1 + c_2\phi_2 + {}_3\phi_3 \qquad\qquad 3.12$$

The coefficients c_j are found from the solution of the matrix equation:

$$G\underset{\sim}{c} = \underset{\sim}{\ell} \qquad\qquad 3.13$$

where the Gramm's matrix G has elements: $g_{kj} = <\phi_k, \phi_j>$
$$j,k=1,\ldots 3$$
and the vector ℓ has elements: $\ell_k = <\Delta g, \phi_k>$
The weight function in the scalar products is given by:

$$W(x_i, y_i) = \sigma_{\Delta g_i}^{-2} \qquad\qquad 3.14$$

The inner zone yields most of the information concerning the influence of local variations in the components of the deflection and it is critically important that there be sufficient well-distributed data in this zone in order to get a reliable estimate of the deflections. Consequently, several criteria have been set up to ensure that the data does have these characteristics. Sufficiency is ensured when there are at least four data points in the region. The distribution is checked by ensuring that there is at least one data point in at least three of the four quadrants around the computation point. This procedure has the disadvantage that for a computation point on the edge of the block, this criterion cannot be satisfied. Some future refinement should be attempted. If these criteria are not met, no deflection components are computed for that point.

(iv) Propagation of Errors

It has been shown(e.g. Heiskanen & Moritz, 1967) that gravity anomalies are correlated with each other as a function of distance, and much research has been done into the representation of this correlation by means of auto-covariance functions and empirical covariance matrices (e.g. Kaula, 1957, Lauritzen, 1973). However, the practical problems involved in using the necessarily large covariance matrices associated with the anomalies have not been successfully overcome. Consequently, for the purpose of this report, the gravity anomalies, both point and mean, have been assumed to be uncorrelated. The propagation of errors for the components ξ_1, ξ_2, η_1, η_2 is then fairly straight-forward:

$$\sigma_{\xi_j} = \frac{1}{4\pi G} \sqrt{[\sum_i (\ (\frac{dS(\psi)}{d\psi})_i \ \cos \ \phi_i \cos \ \alpha_i d\phi_j d\lambda_j)^2 \sigma^2_{\Delta g_i}}$$

$$3.8$$

$$\sigma_{n_j} = \frac{1}{4\pi G} \sqrt{[\ \sum_i (\ (\frac{dS(\psi)}{d\psi})_i \cos \ \phi_i \sin \ \alpha_i d\phi_j \ d\lambda_j)^2 \cdot \sigma^2_{\Delta g_i}}$$

$$\text{for } j = 1, 2$$

The propagation of errors for the inner zone proceeds in two steps. The error covariance matrix of the coefficients is derived from:

$$\Sigma_c = \sigma_o^2 \ G^{-1} \qquad\qquad 3.15$$

where:

$$\sigma_o^2 = \frac{\sum_{i=1}^{n} (\ \Delta g_i - \widetilde{\Delta g}_i)^2 \cdot W(x_i, y_i)}{n-3} \qquad\qquad 3.16$$

The variances of ξ_3 and n_3 are given by:

$$\sigma^2_{\xi_3} = \underset{\sim}{d}_1 \Sigma_c \ \underset{\sim}{d}_1^T$$

$$3.17$$

$$\sigma^2_n = \underset{\sim}{d}_2 \Sigma_c \ \underset{\sim}{d}_2^T$$

where $\underset{\sim}{d}_1$ and $\underset{\sim}{d}_2$ are the linear operators on Δg_p, g_x, g_y in equation 3.9. That is:

$$\underset{\sim}{d}_1 = \{-\frac{1}{2\pi G} \ f_1 - \frac{3}{4\pi GR} \ g_1; \ - \frac{1}{2\pi G} \ f_2 - \frac{3}{4\pi GR} \ g_2; \ - \frac{1}{2\pi G} \ f_3 - \frac{3}{4\pi GR} \ g_3\}$$

$$3.18$$

$$\underset{\sim}{d}_2 = \{- \frac{1}{2\pi G} \ f_1' - \frac{3}{4\pi GR} \ g_1' \ ; \ - \frac{1}{2\pi G} \ f_3' - \frac{3}{4\pi GR} \ g_3' \ ; \ - \frac{1}{2\pi G} \ f_2' - \frac{3}{4\pi GR} \ g_2'\}$$

As stated earlier, the complete gravimetric deflections at one point are then given by:

$$\xi^G = \xi_1 + \xi_2 + \xi_3$$

$$3.4$$

$$n^G = n_1 + n_2 + n_3$$

and estimates for their standard errors $\sigma_{\xi}G$, $\sigma_{\eta}G$ are:

$$\sigma_{\xi}G = \sqrt{(\sigma^2_{\xi_1} + \sigma^2_{\xi_2} \quad \sigma^2_{\xi_2})}$$

$$3.19$$

$$\sigma_{\eta}G = \sqrt{(\sigma^2_{\eta_1} + \sigma^2_{\eta_2} + \sigma^2_{\eta_3})}$$

(v) Choice of Boundaries of Zones

The contribution of each of the three zones used will be a function of the size of each zone. The inner zone, using point gravity data, should be as small as possible, but for practical reasons mentioned earlier, the smallest viable block is one with sides of $1/3°$. The limits for the middle zone, using ($1/3° \times 1/3°$) mean anomalies, and the outer zone, ($1° \times 1°$) means, need to be selected. As we have already shown in the case where interpolated astrogeodetic deflections are required, it is unnecessary to continue the summation of the outer zone to cover the entire earth. Instead a limiting integration distance is chosen, and data beyond this distance from the computation point, neglected. The effect of this distant data is not negligible but, provided the effect varies linearly or near-linearly between computation points in a region, it can be compensated for when interpolating astro-geodetic deflections. For nine well-distributed test points in New Brunswick, the integration distances were varied from 250 km to 600 km in 50 km steps. The root mean square (RMS) difference in the deflections (when compared to the deflections for 600 km integration distance) is shown in figure 3.5. The entire trend is near-linear so that a some-

Fig. 3.5   Variation in deflection values

as a function of integration distance

RMS difference - in arc seconds

Integration Distance - in kms

Fig. 3.6   Variation in deflection values
as a function of area covered
by 1/3° x 1/3° blocks

Size of area covered by 1/3° x 1/3° blocks – in degrees
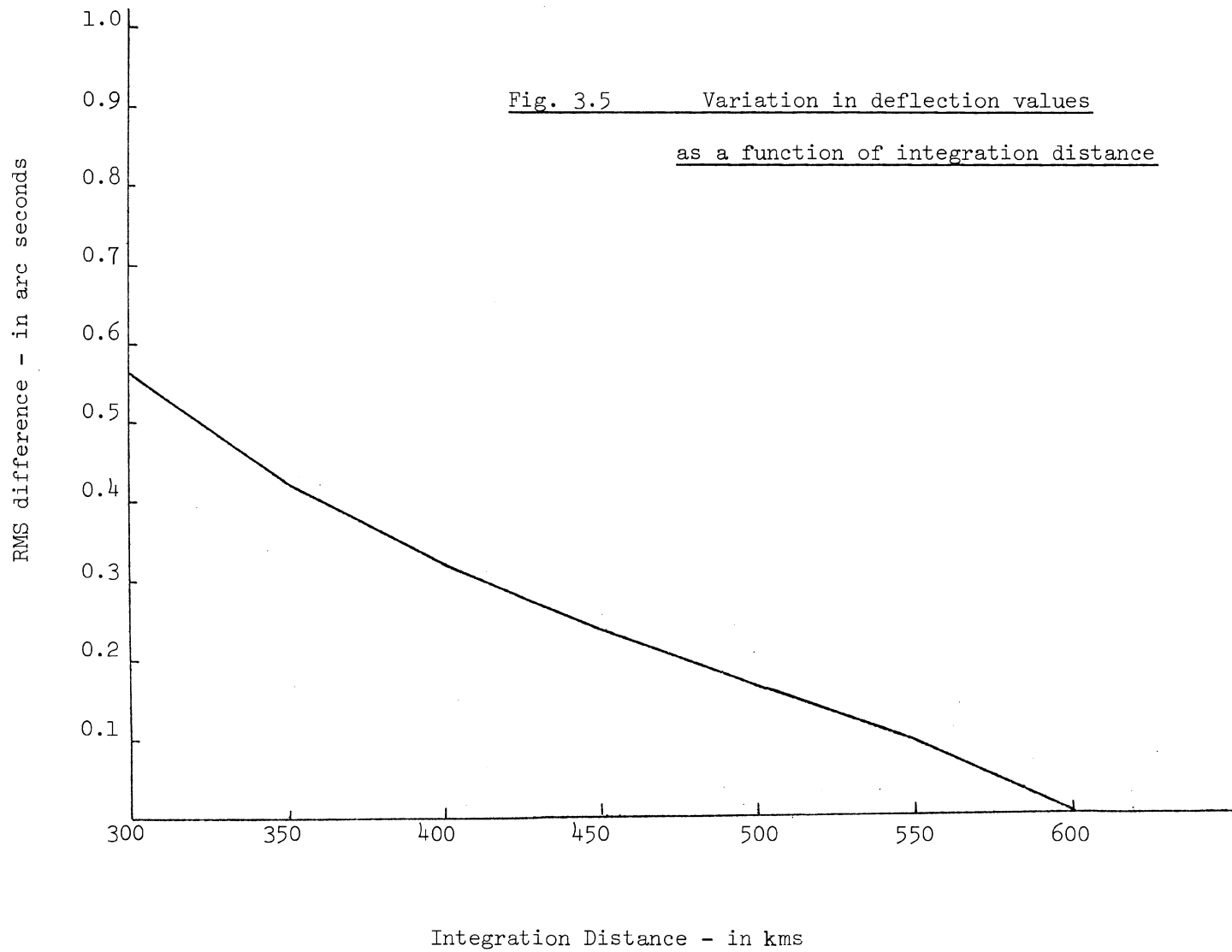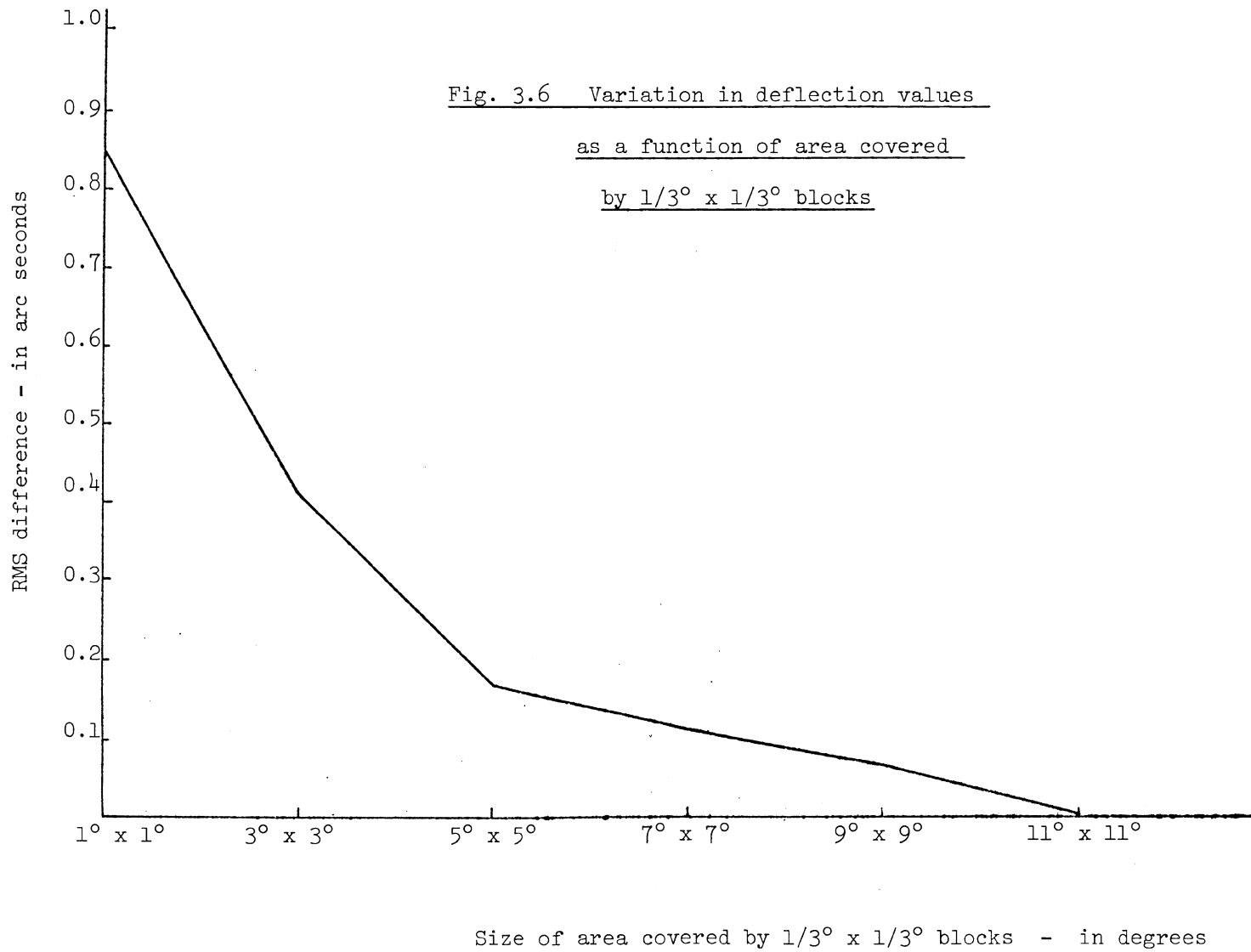
what arbitrary choice of 500 km for the integration distance is justified.

The final limit that must be chosen is that for the middle zone. Obviously, the use of a smaller element size than (1° x 1°) throughout the integration is preferable, but for practical reasons (mainly time of computation) the area covered by 1/3° x 1/3° should be as small as possible. For the same nine test points, the area covered by the (1/3° x 1/3°) blocks has been varied from (1° x 1°) to (11° x 11°) in steps of 2°. The RMS differences, based on the (11° x 11°) deflection values, are shown in figure 3.6. A noticeable change in trend occurs near the (5° x 5°) value on this graph, and this appears to be the minimum area that should be covered by (1/3° x 1/3°) blocks of data, without sacrificing too much accuracy. Consequently, (5° x 5°) has been selected as the area to be covered by the (1/3° x 1/3°) blocks of mean gravity anomalies.

(vi) Curvature of the Plumbline

Gravimetric deflections have been computed for selected regions in New Brunswick, and these have been used to first test the interpolation procedure described in chapter five, and then compute an astrogravimetric geoid for New Brunswick, described in chapter six.

These deflections could also be used for correcting direction and azimuth observations made at the surface of the earth. However, it should be borne in mind that these deflections have been computed at the geoid and are not strictly valid for the terrain. The difference between the two types of deflection (curvature of the actual plumbline)

will be mainly due to topographic irregularities and crustal density anomalies. Investigations in the Alps have shown that the curvature of the plumbline in mountainous terrain can reach 11" (Kobold and Hunziker, 1962).

Consequently, for a rigorous determination of surface deflections, both irregularities in the terrain and density variations should be taken into account. Various methods have been suggested for computing the curvature of the plumbline (Heiskanen and Moritz, 1967), but they will require a detailed topographic survey and a gravity or geological survey in the region of the deflection station. For Canadian conditions, where these surveys are not readily available, further investigations into a more viable approach should be made.

4) <u>Observed Astrogeodetic Deflections</u>

An astrogeodetic deflection of the vertical differs from a gravimetric deflection only in that the ellipsoid used is generally one of different size, shape and orientation. In Canada, the ellipsoid used is the Clarke 1866 ellipsoid which is the reference body used for the North American geodetic networks (Jones 1973).

The astrogeodetic deflection components at a point are given by:

$$\xi^A = \Phi - \phi$$
$$\eta^A = (\Lambda - \lambda) \cos \phi$$

4.1

where (Φ, Λ) are the astronomic latitude and longitude of the deflection station, and (ϕ, λ) are the corresponding geodetic quantities.

Longitude is measured positive eastwards. The above definitions are
only valid if the minor axis of the reference ellipsoid is parallel
to the mean rotation axis of the earth, and the Greenwich meridian
plane of the geodetic system is parallel to the astronomic Greenwich
meridian plane. If this is not the case, the deflections should be
corrected for the rotations between the two systems. There have been
several attempts to determine these rotations (e.g. Lambeck, 1971,
Mueller et al 1972), with some small rotations being evident. An
apparent rotation between the Greenwich meridian planes has been
documented, and is due to the redefinition of the Greenwich mean
astronomic meridian by the Bureau International de l'Heure in 1962
(Stoyko, 1962). This resulted in the longitude of the U.S. Naval
Observatory changing by 0".765, while that of the Dominion Observatory
did not alter. However, in order to avoid the resultant discontinuity
in longitude values, all post-1962 longitudes are still referred to
the old Greenwich mean meridian (D.A. Rice, personal communication).
At some future stage, it will be advisable to use the new Greenwich
mean meridian, especially as satellite-based survey systems are referred
to this meridian. For the purpose of this report, which is to investi-
gate a technique, rather than to obtain a reliable geoid for Canada,
the deflections used have been those calculated from equations 4.1,
and referred to the pre-1962 Greenwich mean astronomic meridian.

Approximately 870 astrogeodetic deflections have been observed
in Canada by the Geodetic Survey of Canada (up to 1972), 151 of these
being either second-order or preliminary values; 3050 deflections

have been observed in the United States of America by the National

Geodetic Survey. At some of these stations, only one component of

the deflection has been determined. The errors in these deflections

are due both to errors in the astronomic co-ordinates and in the

geodetic co-ordinates. Estimates of standard errors of these

deflections have been made, based upon the analysis in (Vaniček and

Merry, 1973). A general model for the errors is:

$$\sigma_\xi = \sqrt{(\sigma_o^2 + \sigma_c^2 + \sigma_p^2 + \sigma_G^2)}$$

$$\sigma_\eta = \sqrt{(\sigma_o^2 + \sigma_c^2 + \sigma_p^2 + \sigma_G^2 + \sigma_T^2)}$$

4.2

where: σ_o is an estimate for the observing precision (0".5 and 0".6

for Φ and Λ, respectively); σ_c is an estimate of the effect of systematic

differences between star catalogues (0".4 for older observations, 0".0

for recent observations); σ_p represents the maximum error due to polar

motion (0".2 and 0".2 tan ϕ for ξ, and η); σ_G is the effect of random

errors in the geodetic co-ordinates ($\sigma_G = 1.89 \times 10^{-5} \cdot K^{2/3}$; K the

distance in metres from the origin of the NAD27) and is based upon

Simmon's rule-of-thumb (Simmons, 1950); σ_T is an estimate of the error

due to the telegraph timing techniques of the older observations

(1".5 for pre-1925 data, 0".0 for post-1925 data).

For second-order deflections, a value of $\sigma_o = 1$".5 has been

used. After 1962, the American data has been corrected for polar

motion and, for these, $\sigma_p = 0$".0. σ_G does not take into account any

systematic errors in the networks due to scale or adjustment distortions.

Another systematic error that has not been taken into account is that
due to the curvature of the plumbline. The observed deflections have
not been reduced from the terrain to the geoid, and as stated already,
this error may reach values in excess of 10" in mountainous regions
(Kobold and Hunziker, 1962). The astrogeodetic deflection coverage in
Canada is depicted in figure 1.1. This coverage has been concentrated
in the south, where access is easier, and there are many more geodetic
stations on the NAD27. Astrogeodetic deflections in the central and
northern regions can only be obtained by observing at already established
geodetic stations, which primarily limits the deflections to being
established along geodetic triangulation chains, leaving large empty
areas. These areas could be covered by the method outlined in the
next chapter, so that a more homogeneous distribution of astrogeodetic
deflections results.

5) Interpolated Astrogeodetic Deflections

Interpolated "astrogeodetic" deflections, i.e. deflections related to the geodetic reference ellipsoid, are determined from the modified gravimetric deflections ξ^G, η^G by adding to them corrections $\delta\xi$, $\delta\eta$. These corrections are, as we have stated already, due to two causes:

(i) the fact that the gravimetric and astrogeodetic deflections are related to two different ellipsoids, of different size, shape and orientation;

(ii) the fact that the modified gravimetric deflections do not account for the influence of the actual gravity field beyond the outer zone.

The first part, $\delta\xi_1$, $\delta\eta_1$, of the corrections can be expressed analytically [Merry and Vaníček, 1974]:

$$\delta\xi_1 = -\sin\phi\,\cos\lambda\,\frac{\Delta X}{a} - \sin\phi\,\sin\lambda\,\frac{\Delta Y}{a} - \cos\phi\,\frac{\Delta Z}{a} + \cos\lambda\,\delta\psi -$$
$$- \sin\lambda\delta\varepsilon - 2a\,\sin\phi\,\cos\phi\delta f \qquad\qquad 5.1$$
$$\delta\eta_1 = -\sin\lambda\,\frac{\Delta X}{a} + \cos\lambda\,\frac{\Delta Y}{a} - \delta\omega + \sin\phi\,\sin\lambda\delta\psi + \sin\phi\,\cos\lambda\delta\varepsilon$$

where: $(\Delta X, \Delta Y, \Delta Z)$ are the coordinates of the geocentre in a cartesian coordinate system with its origin at the centre of the geodetic ellipsoid, i.e. the so-called translation components, and $(\delta\varepsilon, \delta\psi, \delta\omega)$ are the small rotations necessary to bring the (X, Y, Z) axes in the geodetic system parallel to the corresponding axes of the geocentre. δf is the difference in flattening of the two ellipsoids. If all these quantities were known with sufficient precision, it would be a comparatively simple

matter to transform the gravimetric deflections to astrogeodetic

deflections. However, there still exists uncertainty about the

values of the translation components, which can only be determined

if the geoidal heights are known accurately enough. The rotational

elements determined so far (e.g. Lambeck, 1971) barely rise above the

noise level of the solutions. Consequently, this method does not promise

too much at this stage.

The second part, $\delta\xi_2$, $\delta\eta_2$, of the corrections can be also

evaluated from the existing gravity data from all over the world.

However, it is a tedious process and the level of uncertainty is high.

An alternative approach is to approximate the whole

correction:

$$\delta\xi = \delta\xi_1 + \delta\xi_2, \quad \delta\eta = \delta\eta_1 + \delta\eta_2 \qquad 5.2$$

by two second-order polynomial expressions, the coefficients of which

are empirically found (using the existing astro-deflections):

$$\delta\xi \doteq \tilde{\delta\xi} = \sum_{\substack{i=0 \\ j=0}}^{2} a_{ij}x^i y^j = \sum_{\ell=1}^{9} c_\ell \phi_\ell(x, y)$$

$$5.3$$

$$\delta\eta \doteq \tilde{\delta\eta} = \sum_{\substack{i=0 \\ j=0}}^{2} b_{ij}x^i y^j = \sum_{\ell=1}^{9} c'_\ell \phi_\ell(x, y)$$

where (x, y) form a local orthogonal coordinate system and are given

by:

$$x = \phi - \phi_o$$
$$5.4$$
$$y = \lambda - \lambda_o$$

and (ϕ_o, λ_o) are the latitude and longitude of the centre of the region

for which the interpolation is to be carried out. The coefficients a_{ij}, b_{ij} are found using the least squares approximation technique described earlier:

$$\sum_{\substack{i=0\\j=0}}^{2} <x^k \cdot y^\ell, x^i y^j> a_{ij} = <\delta\xi, x^k \cdot y^\ell>$$

$$k, \ell = 0, 1, 2 \qquad 5.5$$

$$\sum_{\substack{i=0\\j=0}}^{2} <x^k \cdot y^\ell, x^i y^j> b_{ij} = <\delta\eta, x^k \cdot y^\ell>$$

The weighting functions, used in the inner products are:

$$W(\delta\xi) = (\sigma_\xi^2 A + \sigma_\xi^2 G)^{-1}$$

$$W(\delta\eta) = (\sigma_\eta^2 A + \sigma_\eta^2 G)^{-1}$$

Equations 5.5 can be rewritten in matrix form as:

$$G\underset{\sim}{a} = \underset{\sim}{m}$$

$$G\underset{\sim}{b} = \underset{\sim}{n} \qquad 5.6$$

from which:

$$\underset{\sim}{a} = G^{-1} \underset{\sim}{m}$$

$$\underset{\sim}{b} = G^{-1} \underset{\sim}{n} \qquad 5.7$$

The error covariance matrices of the coefficients are found from:

$$\Sigma_a = \sigma_{oa}^2 \, G^{-1}$$

$$\Sigma_b = \sigma_{ob}^2 \, G^{-1} \qquad 5.8$$

where:

$$\sigma^2_{oa} = \frac{\sum\limits_{i=1}^{n} (\delta\xi_i - \hat{\delta\xi}_i)^2 \; W(\delta\xi_i)}{n-9}$$

$$\sigma^2_{ob} = \frac{\sum\limits_{i=1}^{n} (\delta\eta_i - \hat{\delta\eta}_i)^2 \; W(\delta\eta_i)}{n-9}$$

5.9

n = number of astro-deflections used for computing the corrections. The error covariance matrices of the quantities $\tilde{\delta\xi}$, $\tilde{\delta\eta}$ are:

$$\Sigma_{\hat{\delta\xi}} = C\Sigma_a C^T$$

$$\Sigma_{\tilde{\delta\eta}} = C\Sigma_b C^T$$

5.10

where C is the matrix

$$C = \begin{bmatrix} \phi_1(x_1, y_1) & \phi_2(x_1, y_1) & \cdots\cdots & \phi_9(x_1, y_1) \\ \phi_1(x_2, y_2) & \phi_2(x_2, y2) & \cdots\cdots & \phi_9(x_2, y_2) \\ \vdots & & & \\ \phi_1(x_n, y_n) & \phi_2(x_n, y_n) & \cdots\cdots & \phi_9(x_n, y_n) \end{bmatrix}$$

5.11

Here $\phi_i(x, y)$ have the same meaning as in equation 5.3 and n is the number of points for which the corrections $\tilde{\delta\xi}$, $\tilde{\delta\eta}$ are evaluated.

The $\delta\epsilon$, $\delta\eta$ used in equations 5.5 and 5.9 are computed as differences of the observed astrogeodetic deflections, and the modified gravimetric deflections calculated at the same points. This particular method does then require that there be a well-distributed set of observed astrogeodetic deflections, as "control points", in the region of interest. This disadvantage, however, is more than offset by the fact that equations 5.3, besides modelling the part

given by 5.1, can also be used to model the effects of neglecting the

distant zones in the integration for the gravimetric deflection (see

chapter 3). That is, the integrations in the Vening-Meinesz formula

over the entire earth, which would be otherwise necessary, need only

be carried out to such a distance that the effects of the distant zones

will vary in a near-linear fashion across the region of interest. The

selection of this optimum distance has already been discussed in

chapter three.

The corrections, $\tilde{\delta\xi}$, $\tilde{\delta\eta}$, which are functions of the local

coordinates (x, y), can then be estimated for any point in the inter-

polation region. Adding these quantities to the gravimetric deflections,

ξ^G, η^G, the interpolated astrogeodetic deflections are:

$$\hat{\xi}^A = \xi^G + \hat{\delta\xi}$$

$$\hat{\eta}^A = \eta^G + \hat{\delta\eta}$$

5.12

The selection of the astrogeodetic data to be used for the

interpolation forms an integral part of the developed system of auto-

mated deflection interpolation. The following procedure has been

adopted: The limits of the "rectangular" region of interest $(\phi_{max}, \phi_{min},$

$\lambda_{max}, \lambda_{min})$ are determined from the maximum and minimum values of the

latitudes and longitudes of the required interpolated deflections.

Observed astrogeodetic deflections which fall within these

limits, and $0°.5$ outside these limits, are automatically selected.

The distribution of these selected deflections is then tested

to ensure that the interpolated deflections are surrounded by the observed

deflections, i.e. that we deal with interpolation and not extrapolation. This is achieved if there is at least one astrodeflection station in each corner of the region (i.e. in each shaded region in figure 5.1).

Region containing

all data points
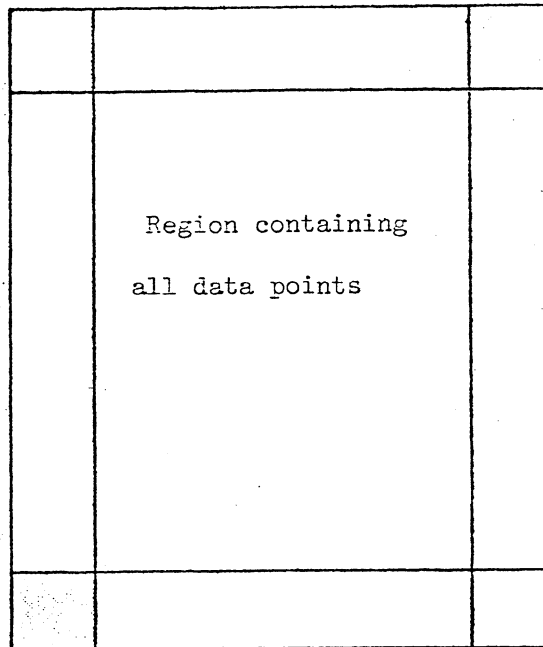
Fig. 5.1 Selection of Astrogeodetic data

If this criterion is not satisfied the search area for the observed astro-deflections is enlarged by $0°5$ again. If there are still insufficient observations in the corners, the whole procedure is repeated. If, after five attempts, the criterion is not satisfied, the interpolation is proceeded with, but the results should be treated with caution.

As a safeguard, both the control points (i.e. the astro-deflection stations) and data points (i.e. gravity stations) should be plotted and the data points checked to ensure that they fall within the bounds defined by the control points.

The procedures described above have been tested in New Brunswick, where deflections were interpolated at 18 points where astro-deflections were known but not used. The control points used, and the 18 data points are shown in figure 5.2. The pertinent data is listed in tables 5.1a and 5.1b.

The interpolated deflections have been compared to the observed deflections at each point. The RMS difference is $2\rlap{.}''14$ in ξ and $1\rlap{.}''74$ in η.

These two anomalously high differences need some explanation. We believe that the $5\rlap{.}''10$ in η (point no. 37) is probably caused by the influence of a few erroneous gravity values in this area, that leaked into the gravity data file. It is recommended that before the geoid is computed in earnest, these errors in the data files be carefully ironed out. The $5\rlap{.}''27$ in ξ (point no. 65) is probably due to the gap in the gravity coverage in the Bay of Fundy. Further refinement of the admittance criteria for individual interpolated deflections is required to deal with these cases. The rest of the differences are smaller than 4".

The vectorial differences, predicted-observed, are shown graphically in fig. 5.3. Estimates of the standard errors of these predicted values have been made, based upon the models described earlier. These range in magnitude from $0\rlap{.}''47$ to $1\rlap{.}''40$. These values

Fig. 5.2 Distribution of control and data points

$\triangle$ - control points

$\bigcirc$ - data points

Point No.	ϕ (deg.)	λ (deg.)	ξ^A (sec.)	$\tilde{\xi}^A$ (sec.)	$\tilde{\xi}^A - \xi^A$ (sec.)	$\sigma_{\tilde{\xi}A}$ (sec.)
45	46.556	66.122	-1.40	-1.31	+0.09	0.75
49	45.962	66.638	-1.42	-1.76	-0.34	0.67
37	47.097	65.735	-0.18	-0.12	+0.06	1.07
41	46.120	67.110	-2.20	-6.09	-3.89	0.80
50	46.243	65.852	-0.20	-1.10	-0.90	0.54
57	46.042	66.490	-1.16	-3.06	-1.90	0.66
58	47.003	65.575	-0.07	-2.62	-2.55	0.58
62	46.732	65.428	-0.65	-0.53	+0.12	0.51
38	47.622	65.655	-2.39	-0.25	+2.14	0.57
39	47.292	65.622	+2.64	+1.78	-0.86	0.57
47	47.513	67.283	+1.42	+0.07	-1.35	0.69
53	45.750	66.983	-2.04	-1.72	+0.32	0.87
56	46.083	64.790	-0.31	+1.44	+1.75	0.47
59	45.640	65.727	-0.36	+2.68	+3.04	0.56
61	46.958	64.840	+0.08	-0.06	-0.14	0.52
64	46.442	64.858	+3.23	+3.05	-0.18	0.47
65	45.277	66.065	-3.75	+1.52	+5.27	0.72
66	47.205	67.882	+1.61	-1.33	-2.94	0.73

Table 5.1a. Interpolation of Deflections in New Brunswick

- ξ-component.

Point No.	η^A (sec.)	$\tilde{\eta}^A$ (sec.)	$\tilde{\eta}^A - \eta^A$ (sec.)	$\sigma_{\tilde{\eta}^A}$ (sec.)
45	-0.20	-2.42	-2.22	0.72
49	-2.70	-2.27	+0.43	0.67
37	-1.61	+3.49	+5.10	1.40
41	-2.30	-1.70	+0.60	0.80
50	-4.10	-4.45	-0.35	0.57
57	-4.02	-4.35	-0.33	0.64
58	-0.08	-0.38	-0.33	0.60
62	-0.80	-0.93	-0.13	0.56
38	+0.12	-0.19	-0.31	0.69
39	+0.68	+0.15	-0.53	0.68
47	-6.14	-5.69	+0.45	0.75
53	-2.94	-3.70	-0.76	0.89
56	-0.98	-1.90	-0.92	0.49
59	-0.82	-3.86	-3.04	0.54
61	+0.78	+1.36	+0.58	0.54
64	-3.78	-3.26	+0.52	0.48
65	-2.14	-3.92	-1.78	0.74
66	-7.19	-4.45	+2.74	0.77

Table 5.1b. Interpolation of Deflections in New

Brunswick - η-component.
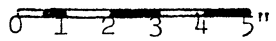
scale of vectors:

0 1 2 3 4 5"

Fig. 5.3 Error vectors (predicted-observed)

appear to be slightly too optimistic and have little correlation with
the actual errors. In investigating why these estimates are too
optimistic the following correlations of the actual errors with:

  (i) horizontal position

 (ii) number of data points in inner zone

(iii) height of station

 (iv) roughness of terrain

were considered. In all but the last, the correlations were insignif-
icant. The correlation of error with roughness of terrain is shown
graphically in fig. 5.4 The correlation coefficient obtained for this
data was 0.34. The measure of the roughness of the terrain was
obtained from the topographic variance, t, given by:

$$t = \frac{\sum\limits_{i=1}^{n} (\bar{H} - H_i)^2}{n} \qquad\qquad 5.13$$

where H_i are the heights of the n measured gravity anomalies in the
inner zone, and $\bar{H}$ is the mean of H_i:

$$\bar{H} = \frac{1}{n} \sum\limits_{i=1}^{n} H_i$$

t is then an indicator of the variation of individual heights in a
region from the mean value. A large value for t indicates rough
terrain, while a small value indicates the converse.

    This correlation is likely to be due mainly to the curvature
of the plumbline. The interpolated deflections will correspond
approximately to deflections at the geoid, as they are based upon
gravimetric data, reduced to the geoid. On the other hand, the astro-
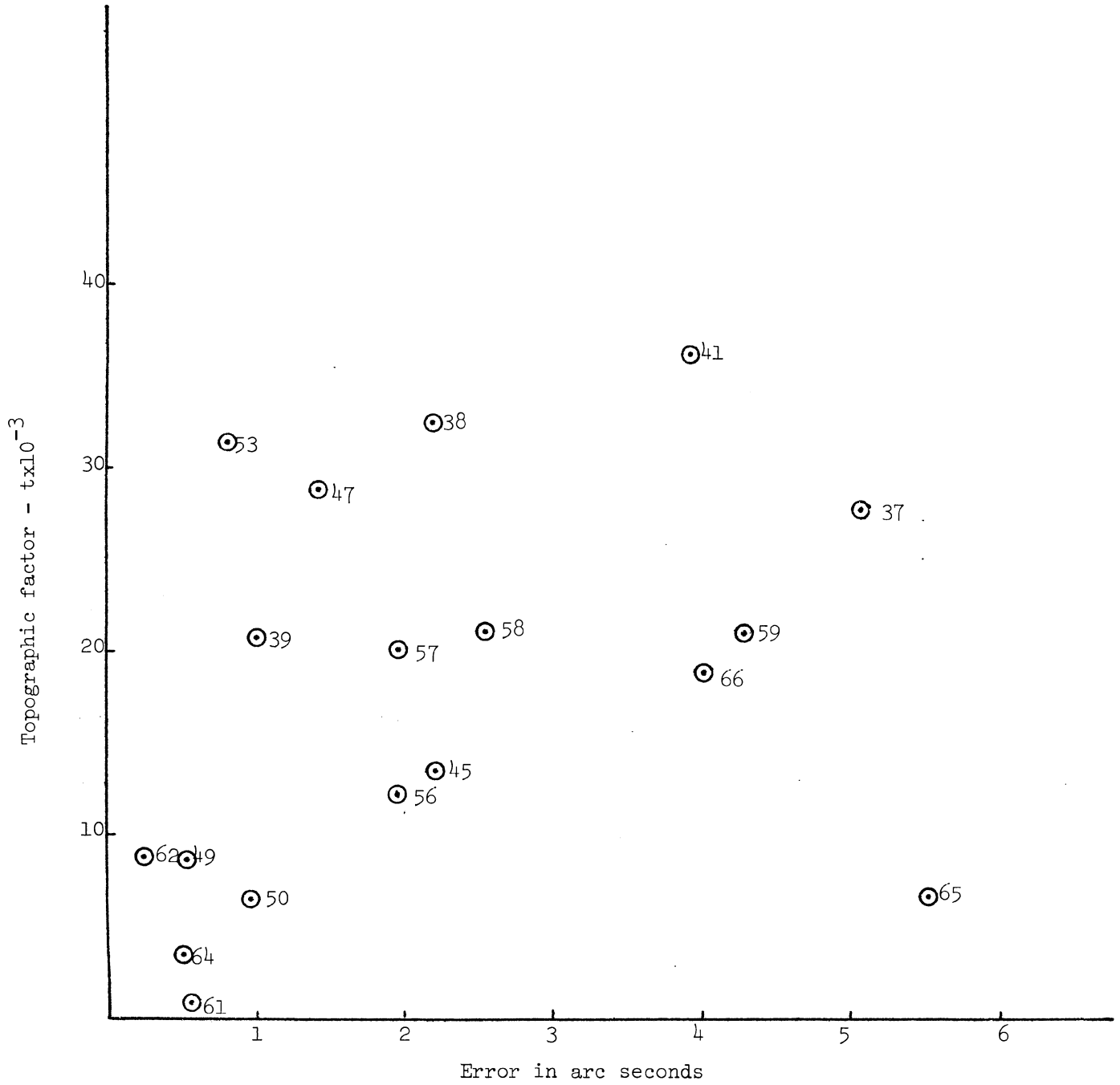
Fig. 5.4 Correlation of Error with Terrain Roughness

geodetic deflections are measured at the surface of the earth. As mentioned previously, the plumbline curvature reaches extreme values in mountainous terrain and in regions of variable crustal density. The t-variance is an indicator of the former. Unfortunately, there is no corresponding indicator of the latter.

In order to obtain more accurate results then, the plumbline curvature should be known and accounted for. This is not easily done, although attempts are being made to develop a model for the curvature [Nydetabula, 1974]. A less satisfactory alternative solution is to scale the estimated standard errors by a factor related to the t-variance (equation 5.13), resulting in more reliable prediction of these errors. Before this can be attempted more investigation is needed into the correlation between the actual errors and the roughness of the terrain.

6) Geoid Computation

Deflections of the vertical represent the slope of the geoid with respect to the reference ellipsoid in two orthogonal directions:

$$\frac{\partial N}{\partial \phi} = -\tan \xi \doteq -\xi$$

6.1

$$\frac{\partial N}{\partial \lambda} \cos \phi = -\tan \eta \doteq -\eta$$

Consequently, it is logical to determine the geoidal height difference between two points P, Q by integrating the deflections along the line PQ:

$$N_Q - N_P = -\int_P^Q (\xi \cos \alpha + \eta \sin \alpha) ds$$

6.2

where N_Q, N_P are the geoidal heights at Q and P and α is the azimuth of the line segment ds. In the classical, Helmert's, approach, the above expression is replaced by:

$$N_Q - N_P \doteq -\frac{1}{2} (\xi_Q \cos \alpha + \eta_Q \sin \alpha + \xi_P \cos \alpha + \eta_P \sin \alpha) s$$

6.3

where s is the distance between P and Q.

The above procedure can be used to calculate changes in geoidal height between adjacent deflection stations, and hence to produce astrogeodetic geoids. Various methods have been derived to use all possible combinations of deflection stations (see, for instance, Ney (1952), Fischer et al (1967) and Lachappelle (1973)). However, all these methods make use of equation 6.3 in some form or other. Thus they are restricted to measuring geoidal profiles along chains of

geodetic triangulation and traverses. The basic assumption is also made that between any two adjacent deflection stations the geoidal height varies linearly.

The method used in this report - surface fitting to the deflections - differs markedly. Linearity in the variation of geoidal height between adjacent stations is not assumed, the technique is not restricted to profiles, and full advantage is taken of the tridimensionality of the geoidal surface [Vaníček and Merry, 1973]. The principal formulae are shown below. (For a complete derivation, refer to the paper which is attached as an external appendix).

The geoidal height, $N(x, y)$ at a point (x, y) is approximated by a polynomial of order n:

$$P_n(x, y) = \sum_{i,j = 0}^{n} C_{ij} \, x^i y^j = N(x, y) \qquad 6\text{-}4$$

where
$$x = R(\phi - \phi_o)$$
$$y = R(\lambda - \lambda_o) \cos \phi \qquad 6\text{-}5$$

R is a mean radius of curvature of the earth, and (ϕ_o, λ_o) is an arbitrary origin of the (x, y) coordinate system. The slope of the geoid in two orthogonal directions is:

$$\frac{\partial P_n}{\partial x} \doteq \frac{\partial N}{\partial x} = -\tan \xi \doteq -\xi$$

$$6\text{-}6$$

$$\frac{\partial P_n}{\partial y} \doteq \frac{\partial N}{\partial y} = -\tan \eta \doteq -\eta$$

The observed values ξ, η which are functions of position, are used to determine the coefficients of the best-fitting polynomial (in the least-squares sense):

$$\sum_{s,r}' [C_{sr}(is < W_\xi x^{s+i-2}, y^{r+j} > + jr < W_\eta x^{s+i}, y^{r+j-2} >)] =$$

6-7

$$= -i < W_\xi\xi, x^{i-1} y^j > -j < W_\eta\eta, x^i y^{j-1} > \text{ for } i, j = 0, \ldots n$$
$$i+j \neq 0$$

The weights W_ξ, W_η are determined from:

$$W_\xi = \sigma_\xi^{-2}A$$

$$W_\eta = \sigma_\eta^{-2}A$$

6-8

where $\sigma_\xi A$, $\sigma_\eta A$ are the given standard deviations of the astro-deflection components. Equation 6.7 may be written, in matrix notation, as:

$$A\underset{\sim}{b} = \underset{\sim}{u}$$

6-9

from which

$$\underset{\sim}{b} = A^{-1}\underset{\sim}{u}$$

6-10

The error covariance matrix of the coefficient vector $\underset{\sim}{b}$ is formed from:

$$\Sigma_b = \sigma_o^2 A^{-1}$$

6-11

where

$$\sigma_o^2 = \frac{\sum_{i=1}^{\ell} [W_{\xi_i} (\frac{\partial P_n}{\partial x}\big|_{\substack{x=x_i \\ y=y_i}} + \xi_i)^2 + W_{\eta_i} (\frac{\partial P_n}{\partial y}\big|_{\substack{x=x_i \\ y=y_i}} + \eta_i)^2]}{2\ell - (n+1)^2 + 1}$$

6-12

For a vector of computed geoidal heights $\underset{\sim}{N}$, equation 6-4 can be written as:

$$\underset{\sim}{N} = B\underset{\sim}{b} \qquad\qquad 6\text{-}13$$

and the error covariance matrix of $\underset{\sim}{N}$ is given by:

$$\Sigma_{N} = B\Sigma_{b}B^{T} \qquad\qquad 6\text{-}14$$

Note that it is also possible to incorporate any direct information on the geoidal height that might become available. Some preliminary investigation on this has been started.

The above procedures have been tested using a selection of data in North America and various orders of polynomials. The consistency of the results as compared to a gravimetric geoid indicates that an accuracy of 3 to 4 metres (relative to the origin of NAD 27) can be achieved for all of the U.S.A. and for the southern regions of Canada, using the existing data [Vaniček and Merry, 1973]. In a comparison with the results of [Fischer et al, 1967] based also on the astro-deflection data an RMS difference of 3.5 metres was obtained, with a mean (systematic) difference of 4 metres. However, the data used by Fischer was observed prior to 1967 and probably differed significantly from that used by Vaniček and Merry. This could be the likely cause of significant systematic difference. See also the more recent paper by Fischer [1971].

Unpublished geoidal heights for 2528 deflections in the U.S.A. were made available by D.A. Rice (personal communication, 1973). The same data was used to determine the coefficients of a 9th order polynomial for the geoid in the U.S.A. using the above described technique. An RMS difference of 2.3 metres and a mean difference of 0.1 metres was obtained from a comparison with   Rice's results.

Here, the differences are likely due to a combination of the smoothing effect of the polynomial fit, the linear assumptions of equation 6.3, and the different weighting schemes employed.

Another 9th degree polynomial for the geoid in the whole of North America has also been produced. The 100 coefficients are given in Table 6.1. This geoid could serve as a basis for more detailed geoidal computations in those regions where there is a need and sufficient observations to warrant it. For these regional geoid calculations the procedure described earlier can be used, with the geoidal height at the regional origin obtained from the continental geoid being held fixed. Geoidal heights from the continental geoid at several points may also be used as constraints, in the same fashion as described earlier. Some further investigation is warranted into the discontinuities that may occur at the edges of regionally-computed geoids, and into the optimum order of polynomial to be used for the continental geoid.

Coeff. Subscript	Value	Coeff. Subscript	Value	Coeff. Subscript	Value	Coeff. Subscript	Value
00	0.0	25	$+0.0261 \times 10^{-1}$	50	$+0.0001 \times 10^{1}$	75	-3.3774×10^{1}
01	-0.0092×10^{-3}	26	-0.4119×10^{-1}	51	$+0.0008 \times 10^{1}$	76	-5.9311×10^{1}
02	$+0.0294 \times 10^{-3}$	27	-0.7427×10^{-1}	52	-0.0006×10^{1}	77	$+15.2964 \times 10^{1}$
03	$+0.0999 \times 10^{-3}$	28	$+0.7308 \times 10^{-1}$	53	-0.0157×10^{1}	78	-7.9666×10^{1}
04	-0.7366×10^{-3}	29	$+2.9798 \times 10^{-1}$	54	-0.0892×10^{1}	79	$+1.3172 \times 10^{1}$
05	$+0.6267 \times 10^{-3}$	30	-0.0017×10^{-1}	55	$+0.2890 \times 10^{1}$	80	-0.0005×10^{1}
06	$+4.1996 \times 10^{-3}$	31	$+0.0067 \times 10^{-1}$	56	$+1.2683 \times 10^{1}$	81	$+0.0138 \times 10^{1}$
07	-6.9850×10^{-3}	32	$+0.0919 \times 10^{-1}$	57	-3.5185×10^{1}	82	$+0.0868 \times 10^{1}$
08	-8.0679×10^{-3}	33	-0.2170×10^{-1}	58	-4.3868×10^{1}	83	-0.3089×10^{1}
09	$+15.5617 \times 10^{-3}$	34	-1.3756×10^{-1}	59	$+13.0112 \times 10^{1}$	84	-1.8833×10^{1}
10	$+0.0069 \times 10^{-3}$	35	$+4.0723 \times 10^{-1}$	60	$+0.0002 \times 10^{1}$	85	$+4.2183 \times 10^{1}$
11	-0.0507×10^{-3}	36	$+6.5350 \times 10^{-1}$	61	$+0.0039 \times 10^{1}$	86	$+9.2322 \times 10^{1}$
12	-0.2474×10^{-3}	37	-24.1848×10^{-1}	62	$+0.0270 \times 10^{1}$	87	-23.7164×10^{1}
13	$+0.3262 \times 10^{-3}$	38	-7.6273×10^{-1}	63	-0.0744×10^{1}	88	$+0.2775 \times 10^{1}$
14	$+4.2500 \times 10^{-3}$	39	$+35.4695 \times 10^{-1}$	64	-0.4344×10^{1}	89	$+30.4644 \times 10^{1}$
15	-7.3124×10^{-3}	40	-0.0001×10^{1}	65	$+0.8991 \times 10^{1}$	90	$+0.0004 \times 10^{1}$
16	-24.7859×10^{-3}	41	-0.0008×10^{1}	66	$+0.0702 \times 10^{1}$	91	-0.0058×10^{1}
17	$+66.1209 \times 10^{-3}$	42	$+0.0022 \times 10^{1}$	67	-0.8299×10^{1}	92	-0.0338×10^{1}
18	$+51.9008 \times 10^{-3}$	43	$+0.0148 \times 10^{1}$	68	$+9.7120 \times 10^{1}$	93	$+0.1388 \times 10^{1}$
19	158.3417×10^{-3}	44	$+0.0705 \times 10^{1}$	69	-20.1897×10^{1}	94	$+0.7852 \times 10^{1}$
20	$+0.0005 \times 10^{-1}$	45	-0.2300×10^{1}	70	-0.0001×10^{1}	95	-1.9057×10^{1}
21	$+0.0031 \times 10^{-1}$	46	-0.4622×10^{1}	71	-0.0123×10^{1}	96	-4.1872×10^{1}
22	-0.0144×10^{-1}	47	$+1.6362 \times 10^{1}$	72	-0.0778×10^{1}	97	$+12.0168 \times 10^{1}$
23	-0.0182×10^{-1}	48	$+0.8128 \times 10^{1}$	73	$+0.2523 \times 10^{1}$	98	$+1.0881 \times 10^{1}$
24	$+0.1063 \times 10^{-1}$	49	-3.5054×10^{1}	74	$+1.5874 \times 10^{1}$	99	-24.1316×10^{1}

Note: Origin at Meades Ranch; (x, y) coordinates scaled by dividing by 4.5×10^{6}

Table 6.1. Coefficients of North American Geoid.

7) <u>Testing and Evaluation</u>

The procedures described in the previous chapters have under-
gone some limited testing in New Brunswick. Lack of funds has
prohibited more extensive testing and evaluation of these techniques,
and the results obtained must be considered as preliminary only.

As mentioned in chapter 5, comparisons indicate that
deflections can be interpolated to an average accuracy of 2" in New
Brunswick at present. It can possibly be improved to 1" to 1.5"
once the technique is refined. The question now arises: "How do
these interpolated deflections improve the computation of the geoid?"
In order to answer this question, deflections were interpolated at
nine points in New Brunswick and a regional (astrogravimetric) geoid,
incorporating these deflections, was computed. This was then compared
to an astrogeodetic geoid, computed without using the interpolated
information. These two geoids were computed using the technique
described in the previous chapter with a 9th degree polynomial and
holding the height of a point near the centre of the region fixed at
3.5 m, the value obtained from the continental solution. The observed
astrogeodetic deflections and the interpolated deflections used are
shown in figure 7.1. The distribution of the interpolated deflections
leaves much to be desired. Unfortunately, this distribution is
practically imposed by the lack of available gravity data in Central
and Northern New Brunswick, about which little can be done at this stage.
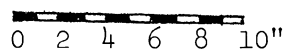
Fig. 7.1 Astrogeodetic and Astrogravimetric deflection stations

    △ - astrogeodetic stations

    ○ - astrogravimetric stations (with deflection vectors)

scale of deflection vectors:

0 2 4 6 8 10"

The two computed geoids differ little from each other, and
only the astrogeodetic geoid has been shown in this report (figure 7.2).
The differences between the two geoids (astragravimetric minus astro-
geodetic) are shown graphically in figure 7.3, and range from -0.25 m
to + 0.15 m. For the entire region, the absolute values of the
differences are smaller than the standard errors associated with the
geoidal height differences. The apparent small size of the differences
is likely to be due to two causes:

  (i) the effect of the comparatively few interpolated deflections would
      be swamped by the effect of the observed deflections.

 (ii) The interpolated deflections are consistent with the general
      slope of the astrogeodetic geoid showing that the distribution
      of masses in the area is rather regular. Thus the interpolated
      deflections tend to support the original "astrogeodetic solution"
      rather than alter it.

It should be noted that the inclusion of the interpolated deflections
resulted in the estimated standard errors of the geoidal heights being
decreased by 5% to 10%. It is conceivable that by including more
interpolated deflections, the accuracy can be further improved.

The differences, which may be considered to be insignificant
in this small region of Canada, where a reasonable quantity of
observed data is available, could become significant for a larger
region. For example, the approximate north-south slope in figure 7.3
of 0.4 m/300 km. would result in a discrepancy of 4 m over a distance
of 3000 km.

Contour labels: 5.0, 1.5, 3.0, 4.0, 2.0, 2.5, 3.5, 4.5, 1.0, 0.5

Fig. 7.2 Astrogeodetic geoid in New Brunswick

(heights in metres)

Fig. 7.3 Astrogravimetric minus Astrogeodetic Geoid in
New Brunswick (in metres)

With the limited results obtained thus far, it would be presumptuous to make any firm conclusions at this stage. However, the following summary may be made:

1) A technique for interpolating astrogeodetic deflections of the vertical has been developed, programmed and tested (for a limited area) with encouraging results.

2) A technique for computing geoidal heights based upon deflections of the vertical (astrogeodetic as well as interpolated) has been developed, programmed, and tested. It appears to be working well.

3) Preliminary testing of the interpolation technique has indicated that an accuracy of the order of 2" may be achieved.

4) The inclusion of interpolated deflections should result in an increased reliability for geoidal heights in Canada and strengthen the solution particularly in areas with little astro-deflection coverage.

Some recommendations may also be made concerning further refinement of the suggested technique:

(1) Further studies should be made into the best practical methods of predicting mean gravity anomalies in unsurveyed areas to produce a reliable and homogeneous gravity data set.

(2) The effect of plumbline curvature should be considered, for two purposes:

(i) to reduce astrogeodetic deflections to the geoid, for calculation of geoidal heights.

(ii) to transfer predicted deflections from the geoid to the terrain,
for azimuth and direction reductions.

Hence a development of a workable technique for computing the cur-
vature correction should be encouraged.

(3) Further investigation is needed into the limitations of the inter-
polation procedure (in, for example, mountainous areas) and into the
means of obtaining more reliable accuracy estimates for the deflections.

(4) The optimum number of interpolated deflections and their dis-
tribution in various areas should be determined.

Through the course of this investigation, it has become
apparent that the gravity coverage in Canada, as made available to us
by the Earth Physics Branch, is not everywhere adequate. It is
likely that the interpolation technique, and consequently the refinement
to the astrogeodetic geoid, will not be useable in several regions of
Canada, due to this reason. Therefore, we recommend that the respon-
sible federal agencies (Earth Physics Branch, Bedford Institute, etc.
be   encouraged to continue to collect and process all available gravity
data (including that from private sources) and to make this data
available to the geodetic community as rapidly as possible.

ACKNOWLEDGEMENTS

REFERENCES

Buck, R.J. and J.G. Tanner (1972). Storage and Retrieval of Gravity
        Data. Bulletin Géodésique, No. 103.

Decker, B.L. (1972). Present day accuracy of the Earth's Gravitational
        Field. Paper presented at Int. Symp. on Earth Gravity
        Models and Related Problems, St. Louis.

Department of Energy, Mines and Resources (1972). Proceedings 2nd
        National Control Survey Conference, Ottawa.

Derenyi, E.E. (1965). Deflections of the Vertical in Central New
        Brunswick. M.Sc. Thesis, Department of Civil Engineering,
        University of New Brunswick, Fredericton.

Fischer, I. (1965). Gravimetric Interpolation of Deflections of the
        Vertical by Electronic Computer. Paper presented to Special
        Study Group 5-29, IAG, Uppsala.

Fischer, I., M. Slutsky, R. Shirley, P. Wyatt (1967). Geoid Charts
        of North and Central America. U.S. Army Map Service Tech.
        Rep. No. 62.

Fischer, I. (1971). Interpolation of Deflections of the Vertical.
        Report of Special Study Group 5-29 to the 15th General
        Assembly, IAG, Moscow.

Heiskanen, W.A. and H. Moritz (1967). Physical Geodesy. W.H. Freeman,
        San Francisco.

Jones, H.E. (1973). Geodetic Datums in Canada. The Canadian Surveyor,
        Vol. 27, No. 3.

Kaula, W.M. (1957). Accuracy of the Gravimetrically Computed
        deflections of the vertical. Transactions of the AGU,
        Vol. 38.

Kobold, F. and E. Hunziker (1962). Communication sur la Courbure
        de la Verticale. Bulletin Géodésique, No. 65.

Krakiwsky, E.J. and D.E. Wells (1971). The Method of Least Squares.
        University of New Brunswick, Department of Surveying
        Engineering Lecture Notes No. 18.

Krakiwsky, E.J. and D.B. Thomson (1974). Combination of Terrestrial
        and Satellite Networks. University of New Brunswick,
        Dept. of Surveying Engineering, Tech. Rep. in prep.

Lachappelle, G. (1974). A Study of the Geoid in Canada. The
        Canadian Surveyor, in press.

Lambeck, K. (1971). The Relations of Some Geodetic Datums to a Global Geocentric Reference System. Bulletin Géodésique No. 99.

Lauritzen, S.L. (1973). The Probabilistic Background of some Statistical methods in Physical Geodesy. Publications of the Danish Geodetic Institute, No. 48.

Merry, C.L. and P. Vaníček (1973). Horizontal Control and the Geoid in Canada. The Canadian Surveyor, Vol. 27, No. 1.

Merry, C.L., D.B. Thomson, Y.C. Yin Shing Yuen (1974). The Effects of Variations in the Gravity Field on some Canadian Geodetic Networks. Paper presented at CIS Annual Meeting, Vancouver.

Merry, C.L. and P. Vaníček (1974). The Geoid and Datum Translation Components. The Canadian Surveyor, March 1974.

Molodenskij, M.S., V.F. Eremeev, M.I. Yurkina (1962). Methods for the Study of the External Gravitational Field and Figure of the Earth. Israel Program for Scientific Translations, Jerusalem.

Moritz, H. (1972). Advanced Least Squares Methods. Ohio State University, Department of Geodetic Science, Report No. 175.

Mueller, I.I., J.P. Reilly, T. Soler (1972). Geodetic Satellite Observations in North America (Solution NA-9). Ohio State University, Department of Geodetic Science, Report No. 187.

Nagy, D. (1963). Gravimetric Deflections of the vertical by digital computer. Publications of the Dominion Observatory, Vol. 27, No. 1.

Nagy, D. (1973). Free Air Anomaly Map of Canada from Piece-wise Surface Fittings over half-degree blocks. The Canadian Surveyor, Vol. 27, No. 4.

Ney, C.H. (1952). Contours of the Geoid for Southeastern Canada. Bulletin Géodésique, No. 23.

Nydetabula, S. (1974). Investigation of Curvature of the Plumbline. M.Sc. Thesis, Dept. of Surveying Engineering, University of New Brunswick.

Rapp, R.H. (1972). A 300 n.m. Terrestrial Gravity Field. Paper presented at 53rd Annual Meeting, AGU, Washington.

Rice, D.A. (1952). Deflections of the Vertical from Gravity Anomalies. Bulletin Géodésique, No. 25.

Stokes, G.G. (1849). On the variation of gravity on the surface of the earth. Trans. Cambridge Phil. Soc. Vol. 8.

Stoyko, A. (1962). Heure Definitive (TU2) des Signaux Horaires en 1962. *Bulletin Horaire, No. 19 (Series G)*.

Uotila, U.A. (1960). Investigations on the Gravity Field and Shape of the Earth. *Ann. Acad. Scient. Fennicae, A. III, 55*.

Vaníček, P., J.D. Boal, T.A. Porter (1972). Proposals for a More Modern System of Heights for Canada. *Surveys and Mapping Branch Tech. Rep. No. 72-3*.

Vaníček, P. and D.E. Wells (1972). The Least-Squares Approximation and Related Topics. *University of New Brunswick, Department of Surveying Engineering Lecture Notes No. 22.*

Vaníček, P. (1973). Introduction to Adjustment Calculus. *University of New Brunswick, Department of Surveying Engineering, Lecture Notes No. 35.*

Vaníček, P. and C.L. Merry (1973). Determination of the Geoid from Deflections of the Vertical Using a Least-Squares Surface Fitting Technique. *Bulletin Géodésique, No. 103*.

Vening-Meinesz, F.A. (1928). A formula expressing the deflection of the plumbline in the gravity anomalies, and some formulae for the gravity field and the gravity potential outside the geoid. *Proc. Koninkl. Ned. Akad. Wetenschap, V. 31(3)*.

APPENDIX A

Derivation of equations for inner zone contribution to the gravimetric

deflections of the vertical

Let the inner zone ($1/3°$ x $1/3°$) limits be given by: ϕ_1, ϕ_2, λ_1, λ_2 ($\lambda_2 > \lambda_1$, $\phi_2 > \phi_1$). The Vening-Meinesz integral is then:

$$\xi_3 = \frac{1}{4\pi G} \int_{\lambda=\lambda_1}^{\lambda_2} \int_{\phi=\phi_1}^{\phi_2} \Delta g \cos \alpha \cos \phi \frac{dS(\psi)}{d\psi} d\phi d\lambda$$

(A1)

$$\eta_3 = \frac{1}{4\pi G} \int_{\lambda=\lambda_1}^{\lambda_2} \int_{\phi=\phi_1}^{\phi_2} \Delta g \sin \alpha \cos \phi \frac{dS(\psi)}{d\psi} d\phi d\lambda$$

where G is the mean gravity, Δg the free-air anomaly, α the azimuth of the line connecting the computation point with the dummy point in the integration and ψ is the angular distance between these two points.

In the inner zone, ψ is small, and $\frac{dS(\psi)}{d\psi}$ approaches infinity. Then, $\frac{dS(\psi)}{d\psi}$ can be approximated by:

$$\frac{dS(\psi)}{d\psi} \doteq \frac{1}{2(\psi/2)^2} + 8\psi - 6 - 3\frac{1 - \psi/2}{\psi} + 3\psi \ln[\psi/2 + (\psi/2)^2] \quad \text{(A2)}$$

In the particular case of a $1/3°$ x $1/3°$ block, $\psi < 0.01$ radians and:

$$\frac{dS(\psi)}{d\psi} \doteq -\frac{2}{\psi^2} - \frac{3}{\psi} \quad \text{(A3)}$$

with a maximum error of 0.03%. In the integration, ϕ, λ, can be replaced by plane rectangular co-ordinates x, y with origin (x_0, y_0) at the computation point. Then

$$dx = Rd\phi$$

$$dy = R \cos \phi d\lambda$$

$$\psi \doteq S/R$$

$$S = \sqrt{(x^2 + y^2)}$$

where R is a mean radius of curvature for the earth. Considering, for the moment, only the ξ-component, and replacing $\cos \alpha$ by x/s we can rewrite equation (A1) as:

$$\xi_3 \doteq -\frac{1}{4\pi G} \int_{y=y_1}^{y_2} \int_{x=x_1}^{x_2} \Delta g \left(\frac{2R^2}{s^2} + \frac{3R}{s}\right) \cos \alpha \, \frac{dxdy}{R^2}$$

(A4)

$$= -\frac{1}{2\pi G} \int_{y=y_1}^{y_2} \int_{x=x_1}^{x_2} [\Delta g \cdot x(x^2+y^2)^{-3/2} + 3/2 \, \Delta g \, \frac{x(x^2+y^2)^{-1}}{R}] \, dxdy$$

Integration of the above expression over the inner zone requires Δg values to be known over the entire zone. This is not generally the case, and Δg at any point in the zone must be approximated. Δg can be written in the form:

$$\Delta g = \Delta g_0 + x g_x + y g_y + \ldots \quad (0) \tag{A5}$$

where Δg_0 is the gravityanomaly at the computation point (x_0, y_0) and

$$g_x = \frac{\partial \Delta g}{\partial x}\Big|_{\substack{x=x_0 \\ y=y_0}}, \qquad g_y = \frac{\partial \Delta g}{\partial y}\Big|_{\substack{x=x_0 \\ y=y_0}}$$

are the horizontal derivatives of the gravity anomalies at the computation point. This approximation uses just these first three terms in the Taylor series and is equivalent to fitting a plane to the gravity anomalies in the inner zone. Then, for the meridian component:

$$\xi_3 = \frac{-1}{2\pi G} \int_{y=y_1}^{y_2} \int_{x=x_1}^{x_2} (\Delta g_0 + x g_x + y g_y)(x(x^2+y^2)^{-3/2} + \frac{3}{2R} x(x^2+y^2)^{-1}) \, dxdy$$

or

$$\xi_3 = -\frac{1}{2\pi G} \sum_{j=1}^{6} I_j \qquad\qquad (A6)$$

where:

$$I_1 = \Delta g_o \iint_A x(x^2+y^2)^{-3/2} \, dxdy$$

$$I_2 = g_x \iint_A x^2(x^2+y^2)^{-3/2} \, dxdy$$

$$I_3 = g_y \iint_A xy(x^2+y^2)^{-3/2} \, dxdy$$

$$I_4 = \frac{3\Delta g_o}{2R} \iint_A x(x^2+y^2)^{-1} \, dxdy$$

$$I_5 = \frac{3g_x}{2R} \iint_A x^2(x^2+y^2)^{-1} \, dxdy$$

$$I_6 = \frac{3g_y}{2R} \iint_A xy\,(x^2+y^2)^{-1} \, dxdy$$

and the integration is carried out for the whole area A of the inner zone. The solution of these integrals is a non-trivial problem and is described below:

$$I_1 = \Delta g_o \int_{y_1}^{y_2} \frac{-dy}{\sqrt{x^2+y^2})} \Big|_{x=x_1}^{x_2} = -\Delta g_o \, \ell n \, (y+\sqrt{(x^2+y^2)}) \Big|_{x=x_1}^{x_2} \Big|_{y=y_1}^{y_2} \quad (A7)$$

$$I_2 = g_x \{ \int_{y_1}^{y_2} \frac{-xdy}{\sqrt{(x^2+y^2)}} + \int_{y_1}^{y_2} \ell n(x+\sqrt{(x^2+y^2)})dy \} \Big|_{x=x_1}^{x_2} \qquad (A8)$$

$$= -g_x x \, \ell n(y+ (x^2+y^2)) \Big|_{x=x_1}^{x_2} \Big|_{y=y_1}^{y_2} + g_x \int_{y_1}^{y_2} \ell n(x+\sqrt{(x^2+y^2)})dy \Big|_{x_1}^{x_2}$$

The second part of this expression is evaluated separately:

$$\int_{y_1}^{y_2} \ell n(x+\sqrt{x^2+y^2}))dy = \int_{y_1}^{y_2} \ell n\, x \, dy + \int_{y_1}^{y_2} \ell n(1+\sqrt{(1+\frac{y^2}{x^2}}))dy$$

$$= y \, \ell n\, x + \int_{y_1}^{y_2} \ell n(1+\sqrt{(1+\frac{y^2}{x^2}}))dy \qquad\qquad (A9)$$

Putting $1 + \dfrac{y^2}{x^2} = t^2$, then $dy = \dfrac{x^2 t\, dt}{x\sqrt{(t^2-1)}}$

and

$$\int_{y_1}^{y_2} \ln(1+\sqrt{(1 + \tfrac{y^2}{x^2})})dy = \int_{y_1}^{y_2} \ln(t+1) \frac{tx}{\sqrt{(t^2-1)}} dt$$

$$= \ln(t+1) \int_{y_1}^{y_2} \frac{tx}{\sqrt{(t^2-1)}} dt - \int_{y_1}^{y_2} \frac{1}{t+1} (\frac{tx\, dt}{\sqrt{t^2-1}}) dt$$

$$= x \ln(t+1) \sqrt{(t^2-1)} \Big|_{y_1}^{y_2} - x \int_{y_1}^{y_2} \frac{\sqrt{(t^2-1)}}{t+1} dt \qquad (A10)$$

Now:

$$\int_{y_1}^{y_2} \frac{\sqrt{(t^2-1)}}{t+1} dt = \int_{y_1}^{y_2} \sqrt{(\tfrac{t-1}{t+1})}dt = \sqrt{(t-1)}\sqrt{(t+1)}\Big|_{y_1}^{y_2} - \int_{y_1}^{y_2} \frac{dt}{\sqrt{(t-1)}\sqrt{(t+1)}}$$

$$= \sqrt{(t-1)}\sqrt{(t+1)}\Big|_{y_1}^{y_2} - \int_{y_1}^{y_2} \frac{dt}{\sqrt{(t^2-1)}} = \sqrt{(t-1)}\sqrt{(t+1)}\Big|_{y_1}^{y_2} - \ln(t+\sqrt{(t^2-1)})\Big|_{y_1}^{y_2}$$

$$(A11)$$

Back-substituting in equation (10):

$$\int_{y_1}^{y_2} \ln(1+\sqrt{(1 + \tfrac{y^2}{x^2})})dy = x[\sqrt{(t^2-1)}(\ln(t+1)-1) + \ln(t+\sqrt{(t^2-1)})]\Big|_{y_1}^{y_2}$$

Substituting for $t = \sqrt{(1 + \dfrac{y^2}{x^2})}$ and rearranging terms:

$$\int_{y_1}^{y_2} \ln(x+\sqrt{(x^2+y^2)})dy = [y \ln(x+\sqrt{(x^2+y^2)})-y + x \ln(y+\sqrt{(x^2+y^2)})-x \ln x]\Big|_{y_1}^{y_2}$$

Substituting in equation (A8):

$$I_2 = g_x\{y \ln(x+\sqrt{(x^2+y^2)})-y-x \ln x\}\Big|_{x=x_1}^{x_2}\Big|_{y=y_1}^{y_2} \qquad (A8)$$

The evaluation of the third integral is straightforward:

$$I_3 = g_y \int_{y_1}^{y_2} \frac{-y\, dy}{\sqrt{(x^2+y^2)}} \Big|_{x=x_1}^{x_2} = -g_y \sqrt{(x^2+y^2)}\Big|_{x=x_1}^{x_2} \Big|_{y=y_1}^{y_2} \qquad (A12)$$

Further:

$$I_4 = \frac{3\Delta g_0}{4R} \int_{y_1}^{y_2} \ln(x^2+y^2)dy \Big|_{x_1}^{x_2}$$

$$= \frac{3\Delta g_0}{4R} \left\{ y \ln(x^2+y^2) - y + x \arctan \frac{y}{x} \Big|_{x=x_1}^{x_2} \Big|_{y=y_1}^{y_2} \right. \qquad (A13)$$

$$I_5 = \frac{3g_x}{2R} \int_{y_1}^{y_2} (x-y \arctan \frac{x}{y})dy \Big|_{x=x_1}^{x_2}$$

$$= \frac{3g_x}{2R} \left\{ xy \Big|_{y_1}^{y_2} - \int_{y_1}^{y_2} y \operatorname{arccot} \frac{y}{x} dy \right\} \Big|_{x_1}^{x_2}$$

$$= \frac{3g_x}{2R} \left\{ xy \Big|_{y_1}^{y_2} - \frac{y^2}{2} \operatorname{arccot} \frac{y}{x} \Big|_{y_1}^{y_2} + \frac{x}{2} \int_{y_1}^{y_2} \frac{y^2}{y^2+x^2}dy \right\} \Big|_{x=x_1}^{x_2}$$

$$= \frac{3g_x}{2R} \left\{ \frac{xy}{2} - \frac{y^2}{2} \operatorname{arccot} \frac{y}{x} + \frac{x^2}{2} \arctan \frac{y}{x} \right\} \Big|_{x=x_1}^{x_2} \Big|_{y=y_1}^{y_2} \qquad (A14)$$

$$I_6 = \frac{3g_y}{2R} \int_{y_1}^{y_2} \frac{y}{2} \ln(x^2+y^2)dy \Big|_{x=x_1}^{x_2}$$

$$= \frac{3g_y}{8R} \left\{ (x^2+y^2)\ln(x^2+y^2)-y^2 \right\} \Big|_{x=x_1}^{x_2} \Big|_{y=y_1}^{y_2} \qquad (A15)$$

(The integral identities used above are taken from:Selby, S.M. (Editor)
Standard Mathematical Tables. Chemical Rubber Company, 1972).
Evaluating the above equations for the indicated limits, the equation
for ξ_3 becomes:

$$\xi_3 = - \frac{1}{2\pi G} (\Delta g f_1 + g_x f_2 + g_y f_3) - \frac{3}{4\pi GR} (\Delta g g_1 + \frac{1}{2} g_x g_2 + \frac{1}{4} g_y g_3) \quad (A16)$$

where:

$$f_1 = \ln(y_2+\sqrt{(x_1^2+y_2^2)})-\ln(y_2+\sqrt{(x_2^2+y_2^2)})-\ln(y_1+\sqrt{(x_1^2+y_1^2)})\ln(y_1+\sqrt{(x_2^2+y_1^2)})$$

$$f_2 = y_2\ln(x_2+\sqrt{(x_2^2+y_2^2)})-y_2\ln(x_1+\sqrt{(x_1^2+y_2^2)})-y_1\ln(x_2+\sqrt{(x_2^2+y_1^2)})+y_1\ln(x_1+\sqrt{(x_1^2+y_1^2)})$$

$$f_3 = \sqrt{(x_1^2+y_2^2)} - \sqrt{(x_2^2+y_2^2)} - \sqrt{(x_1^2+y_1^2)} + \sqrt{(x_2^2+y_1^2)}$$

$$g_1 = \frac{1}{2}(y_2\ln(x_2^2+y_2^2)+y_1\ln(x_1^2+y_1^2)-y_2\ln(x_1^2+y_2^2)-y_1\ln(x_2^2+y_1^2))+ x_2\tan^{-1}\frac{y_2}{x_2} +$$

$$+ x_1\tan^{-1}\frac{y_1}{x_1} - x_2\tan^{-1}\frac{y_1}{x_2} - x_1\tan^{-1}\frac{y_2}{x_1}$$

$$g_2 = x_2y_2-y_2^2\tan^{-1}\frac{x_2}{y_2} + x_2^2\tan^{-1}\frac{y_2}{x_2} - x_1y_2 + y_2^2\tan^{-1}\frac{x_1}{y_2} - x_1^2\tan^{-1}\frac{y_2}{x_1} - x_2y_1+$$

$$+ y_1^2\tan^{-1}\frac{x_2}{y_1} - x_2^2\tan^{-1}\frac{y_1}{x_2} + x_1y_1 - y_1^2\tan^{-1}\frac{x_1}{y_1} + x_1^2 \tan^{-1}\frac{y_1}{x_1}$$

$$g_3 = (x_2^2+y_2^2)\ln(x_2^2+y_2^2)-(x_1^2+y_2^2)\ln(x_1^2+y_2^2)-(x_2^2+y_1^2)\ln(x_2^2+y_1^2)+(x_1^2+y_1^2)\ln(x_1^2+y_1^2)$$

For η_3, a similar equation can be written, where, $\sin \alpha$ is replaced by y/s:

$$\eta_3 = - \frac{1}{2\pi G} (\Delta g f_1' + g_y f_2' + g_x f_3') - \frac{3}{4\pi GR} (\Delta g g_1' + \frac{1}{2} g_y g_z' + \frac{1}{4} g_x g_z')$$

Here, the equations for f_1', f_2', f_3', g_1', g_2', g_3' are identical to those for f_1, f_2, f_3, g_1, g_2, g_3, except that x and y are everywhere inter-changed.

The above analytical expressions for ξ_3, η_3 are correct to within 0.03% for the case where it is sufficient to model the local gravity anomalies by a plane. If a more complex modelling is required, then many additional integrals would have to be evaluated. The density of gravity data presently available does not warrant the additional effort involved.